Au-Ni-Sn System

Liu *et. al*. **[05Liu]** has published an assessment of the data for this system. Slight corrections were made to obtain agreement with the published data and to accommodate the adopted COST 531 binary data.
The liquidus surface is quite complex with many invariant reactions. In addition to the primary solidificaton fields, shown in **Fig. 159**, there is also a very small DHCP primary liquidus surface at the Au-Sn binary edge at a composition x(Sn) of about 0.21, resulting from the reaction P1. This is however shown in **Fig. 162**

References:

[05Liu] Liu, X.-J., Kinaka, M., Takaku, Y., Ohnuma, I., Kainuma, R., Ishida, K.: *J. Electr. Mater.*; 2005, **34**, 670-679.

Table of invariant reactions

T / °C	Reaction type	Phases	Compositions		
			x_{Au}	x_{Ni}	x_{Sn}
888.7	E1	BCC_A2	0.017	0.749	0.234
		LIQUID	0.289	0.580	0.131
		FCC_A1	0.066	0.846	0.088
		NI3SN_LT	0.000	0.750	0.250
880.7	E2	BCC_A2	0.008	0.730	0.262
		LIQUID	0.405	0.375	0.220
		NI3SN2	0.035	0.596	0.369
		NI3SN_LT	0.000	0.750	0.250
764.3	U1	LIQUID	0.486	0.420	0.094
		FCC_A1	0.125	0.819	0.056
		NI3SN_LT	0.000	0.750	0.250
		FCC_A1	0.514	0.456	0.030

559.2	U2	LIQUID	0.769	0.036	0.195
		NI3SN_LT	0.000	0.750	0.250
		NI3SN2	0.067	0.554	0.379
		FCC_A1	0.909	0.024	0.067
524.0	P1	LIQUID	0.790	0.002	0.208
		FCC_A1	0.924	0.001	0.745
		DHCP	0.909	0.000	0.091
		HCP_A3	0.889	0.001	0.110
507.6	U3	LIQUID	0.770	0.017	0.213
		FCC_A1	0.909	0.012	0.079
		NI3SN2	0.086	0.526	0.388
		HCP_A3	0.881	0.006	0.113
453.5	P2	LIQUID	0.269	0.009	0.722
		NI3SN4	0.000	0.437	0.563
		NI3SN2	0.197	0.321	0.482
		AUNI2SN4	0.143	0.286	0.571
314.9	U4	LIQUID	0.260	0.001	0.739
		NI3SN2	0.286	0.214	0.500
		AU1SN	0.428	0.072	0.500
		AUNI2SN4	0.143	0.286	0.571
306.1	U5	LIQUID	0.252	0.001	0.747
		AU1SN	0.434	0.066	0.500
		AUSN2	0.333	0.000	0.667
		AUNI2SN4	0.143	0.286	0.571
296.9	U6	LIQUID	0.118	0.003	0.879
		AUNI2SN4	0.143	0.286	0.571
		AUSN4	0.156	0.044	0.800
		NI3SN4	0.000	0.429	0.571

296.4	U7	LIQUID	0.214	0.001	0.785
		AUNI2SN4	0.143	0.286	0.571
		AUSN2	0.333	0.000	0.667
		AUSN4	0.164	0.036	0.800
283.1	U8	LIQUID	0.698	0.000	0.302
		NI3SN2	0.267	0.276	0.457
		HCP_A3	0.837	0.001	0.162
		AU1SN	0.467	0.033	0.500
230.6	U9	LIQUID	0.003	0.002	0.995
		NI3SN4	0.000	0.425	0.575
		BCT_A5[(a)]	0.000	0.000	1.000
		AUSN4	0.126	0.074	0.800

[(a)]The BCT_A5 composition is almost pure Sn

Phase information

Phase Name	Common Name	Strukturbericht designation/type	Pearson Symbol
AU4NI2SN4	$AuNi_2Sn_4$	…	…

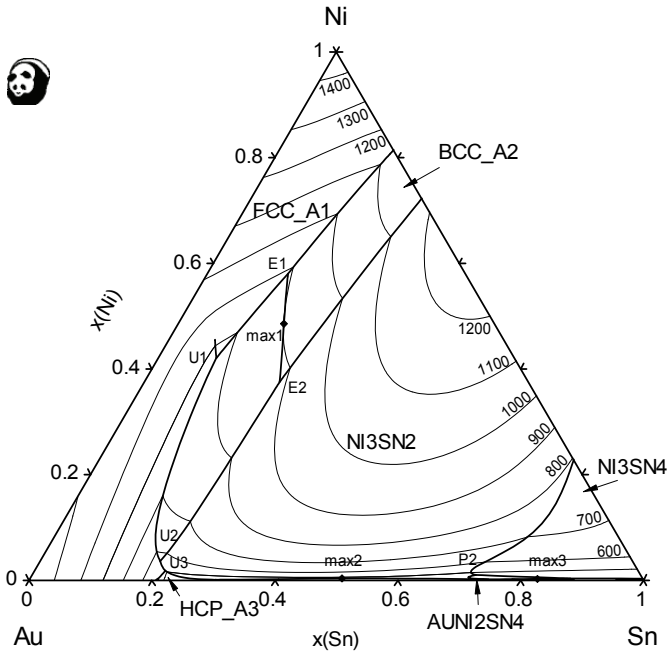

Fig. 159: Liquidus projection of the Au-Ni-Sn system

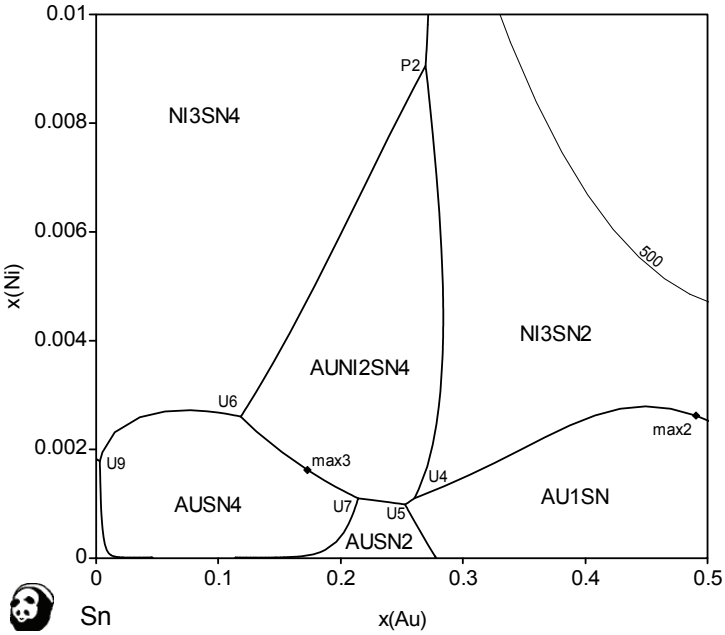

Fig. 160: Liquidus projection in the Sn-rich corner of the Au-Ni-Sn system

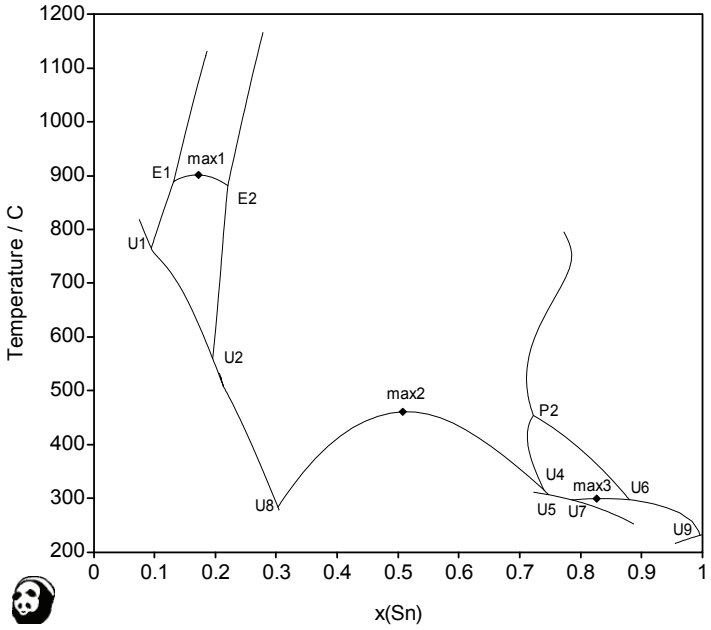

Fig. 161: Liquidus lines in the Au-Ni-Sn system projected onto the T-x(Sn) plane

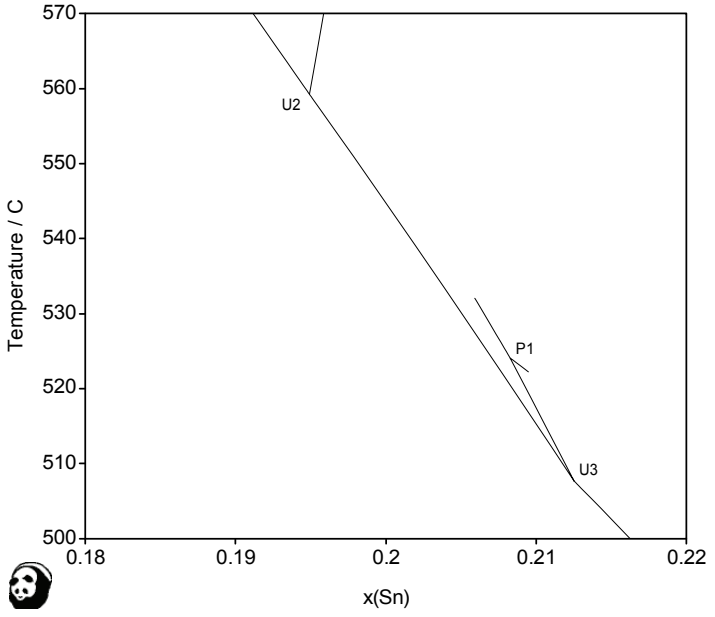

Fig. 162: Magnification of liquidus projection of the Au-Ni-Sn system on the T-x(Sn) plane in the low Sn content

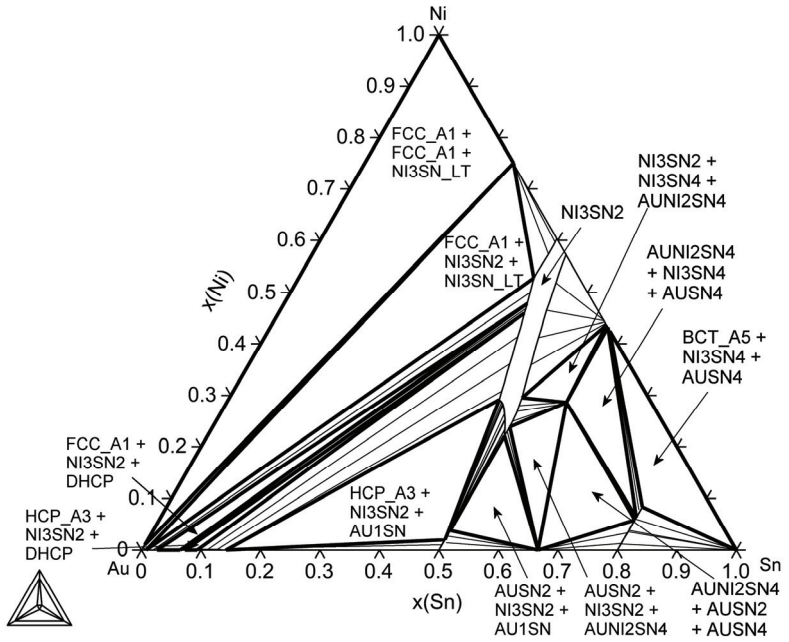

Fig. 163: Isothermal section at 200 °C

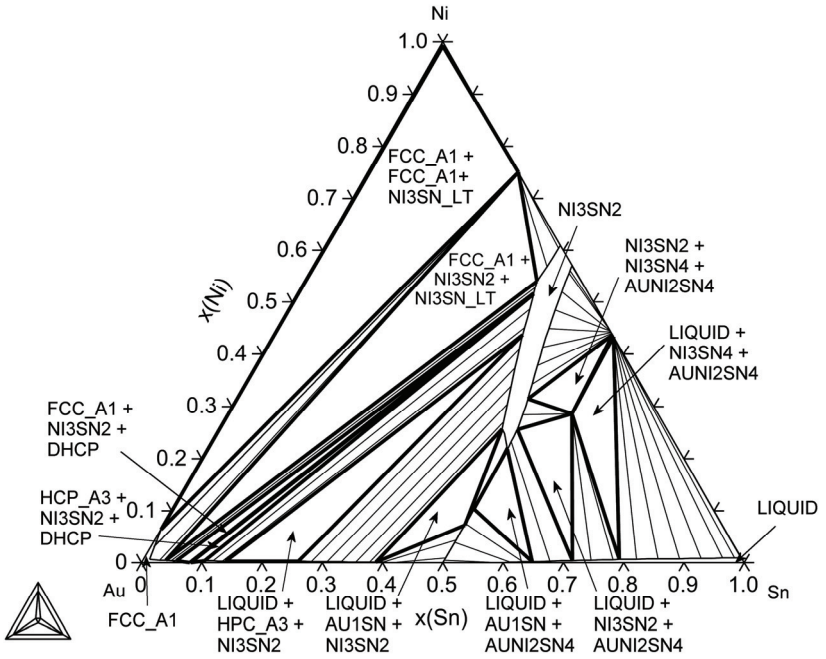

Fig. 164: Isothermal section at 400 °C

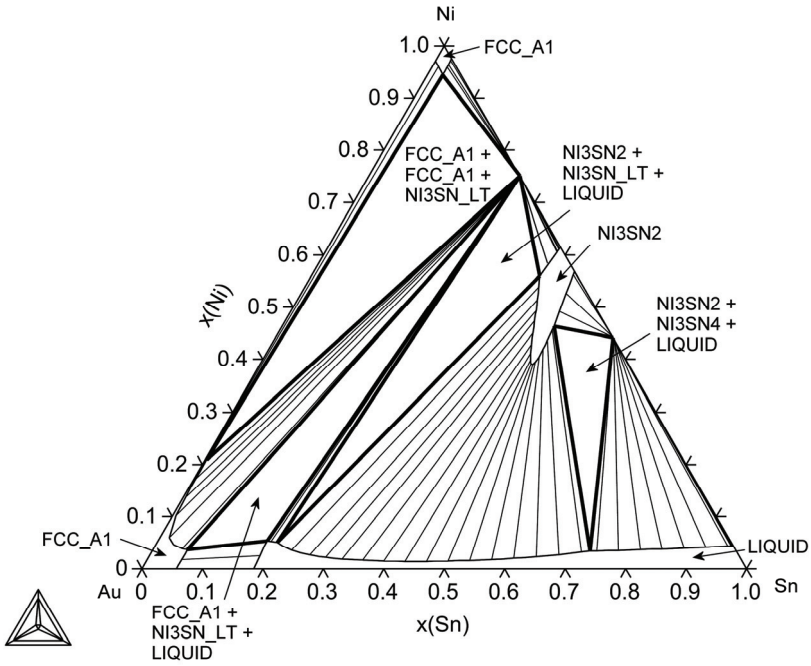

Fig. 165: Isothermal section at 600 °C

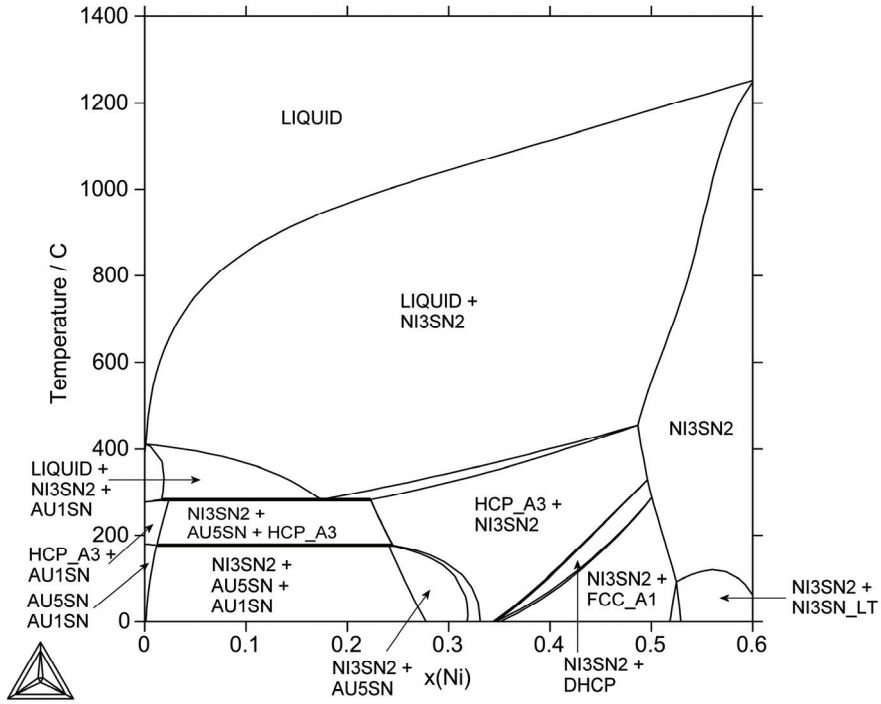

Fig. 166: Isopleth of the Au-Ni-Sn system for 40 at% Sn (close to the invariant point U8)

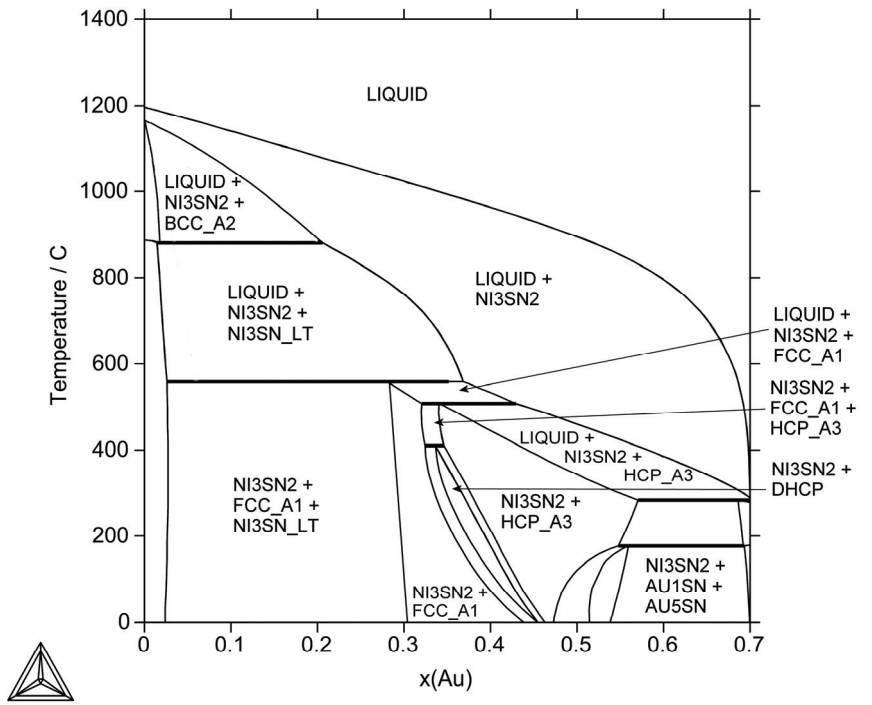

Fig. 167: Isopleth of the Au-Ni-Sn system for 30 at% Sn

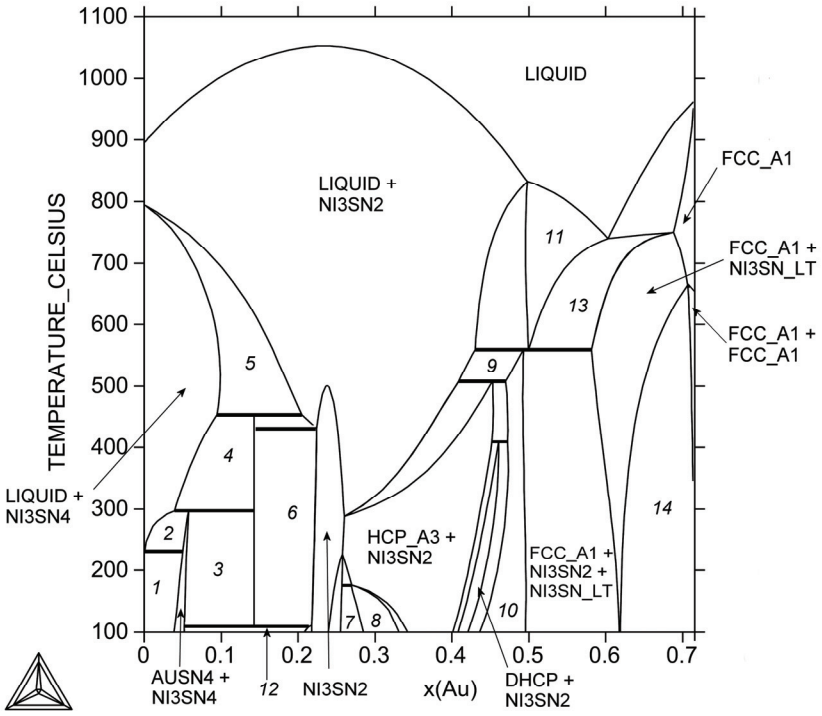

Fig. 168: Isopleth of the Au-Ni-Sn system for 28.6 at% Ni (around the ternary compound)

Legend:

1 – AUSN4+BCT_A5+NI3SN4
2 – LIQUID+ AUSN4 +NI3SN4
3 – AUSN4+ NI3SN4+AUNI2SN4
4 – LIQUID+NI3SN4+AUNI2SN4
5 – LIQUID+NI3SN4+NI3SN2
6 – NI3SN2+AUNI2SN4
7 – NI3SN2+AU1SN+AU5SN
8 – NI3SN2+AU5SN
9 – LIQUID+NI3SN2+FCC_A1
10 – NI3SN2+FCC_A1
11 – LIQUID+NI3SN_LT
12 – AUSN4+NI3SN2+NI3SN4
13 – LIQUID+NI3SN_LT+FCC_A1
14 – NI3SN_LT+FCC_A1+FCC_A1

Bi-In-Sn System

This ternary system was assessed by **[99Yoo]**, but because of changes to the binary data (Bi-In, Bi-Sn, see the part I of this Atlas) it was necessary to reassess the system in the scope of COST 531 Action. The liquidus surfaces in two different projections are shown here, together with selected isothermal sections (near the eutectic temperature) and a set of isopleths (with different ratios of Bi and In near the invariant points E1 and U6) were calculated. The agreement with the experimental data and the previous assessment is very good. Some discrepancies with **[99Yoo]** can be found at the lowest temperatures (below 50 °C), where no experimental data exist.

References:

[99Yoo] Yoon, S. W., Rho, B.-S., Lee, H. M., Kim, C.-U., Lee, B.-J.: *Metall. Mater. Trans.*, 1999, **30A**, 1503-1515.

Table of invariant reactions

T / °C	Reaction type	Phases	Compositions		
			x_{Bi}	x_{In}	x_{Sn}
80.6	U1	LIQUID	0.391	0.402	0.207
		RHOMBO_A7	0.988	0.001	0.011
		BCT_A5	0.109	0.116	0.775
		BIIN	0.500	0.500	0.000
68.3	U2	LIQUID	0.263	0.530	0.207
		BCT_A5	0.058	0.147	0.795
		BIIN	0.500	0.500	0.000
		INSN_GAMMA	0.000	0.219	0.781
65.7	U3	LIQUID	0.206	0.748	0.046
		TET_ALPHA1#1	0.124	0.827	0.049
		BIIN_BRASS	0.333	0.667	0.000
		TETRAG_A6	0.094	0.842	0.064

59.0	U4	LIQUID	0.196	0.666	0.138
		TETRAG_A6	0.076	0.725	0.199
		BIIN_BRASS	0.333	0.667	0.000
		TET_ALPHA1#2	0.071	0.712	0.217
57.3	U5	LIQUID	0.221	0.587	0.192
		BIIN	0.500	0.500	0.000
		BI3IN5	0.375	0.625	0.000
		INSN_GAMMA	0.000	0.210	0.790
55.6	U6	LIQUID	0.207	0.600	0.193
		BI3IN5	0.375	0.625	0.000
		BIIN_BRASS	0.333	0.667	0.000
		INSN_GAMMA	0.000	0.217	0.783
55.3	E1	LIQUID	0.202	0.603	0.195
		TET_ALPHA1#2	0.072	0.617	0.311
		BIIN_BRASS	0.333	0.667	0.000
		INSN_GAMMA	0.000	0.219	0.781

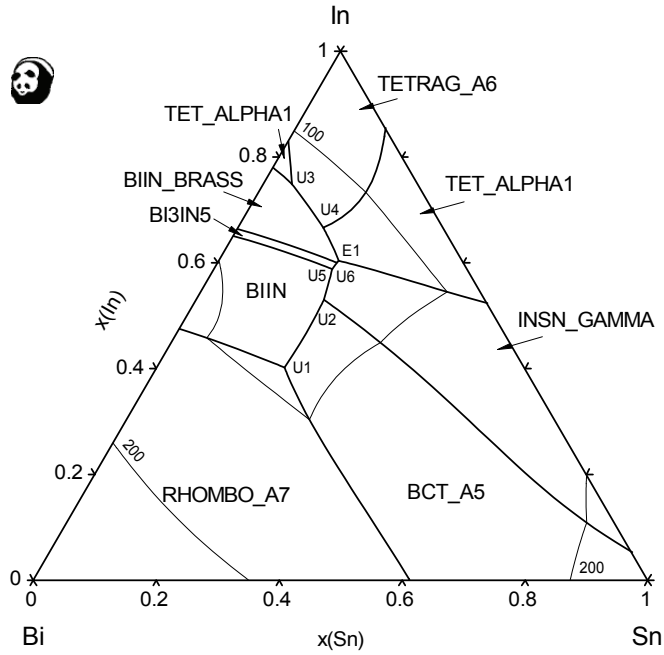

Fig. 169: Liquidus projection of the Bi-In-Sn system

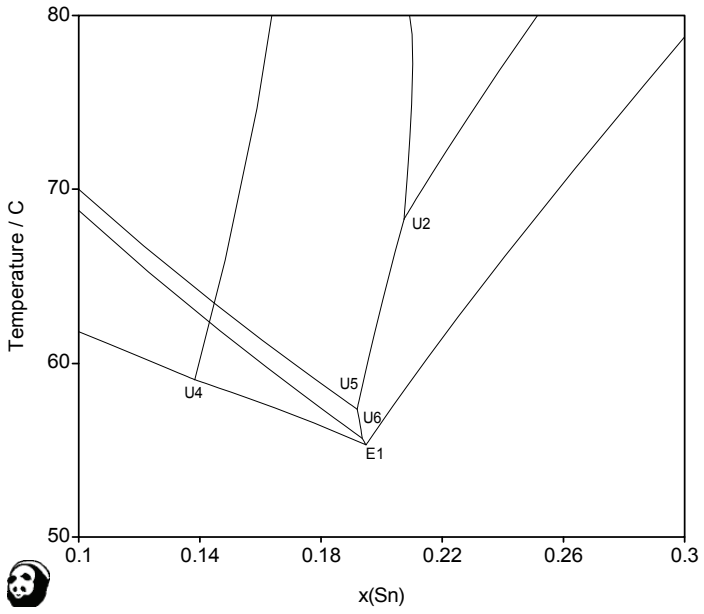

Fig. 170: Liquidus lines in the Bi-In-Sn system in the region of the low-temperature invariants projected onto the T- x(Sn) plane

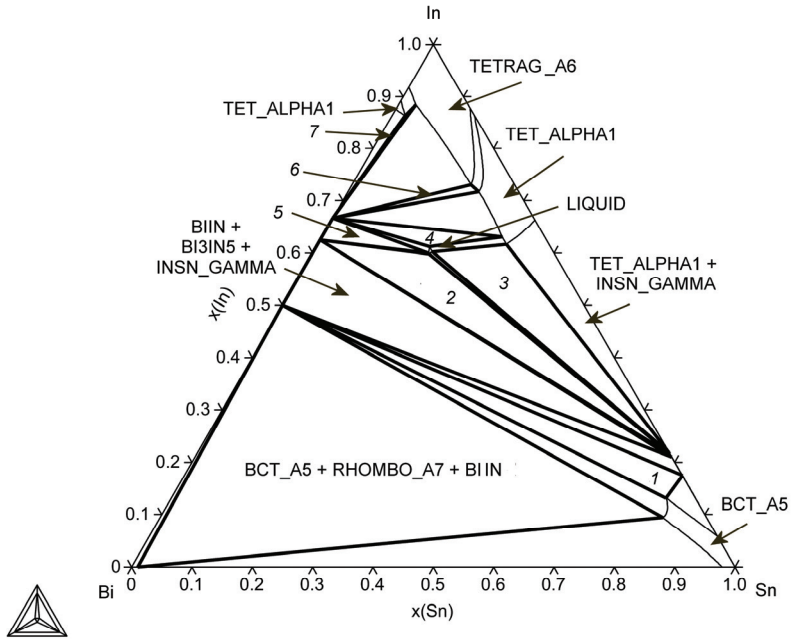

Fig. 171: Isothermal section at 56 °C

Legend:

1 – BCT_A5+BIIN+INSN_GAMMA
2 – LIQUID+BI3IN5+INSN_GAMMA
3 – LIQUID+TET_ALPHA1+INSN_GAMMA
4 – LIQUID+TET_ALPHA1+BIIN_BRASS
5 – LIQUID+BI3IN5+BIIN_BRASS
6 – TET_ALPHA1 +TETRAG_A6+BIIN_BRASS
7 – TET_ALPHA1+TETRAG_A6+BIIN_BRASS

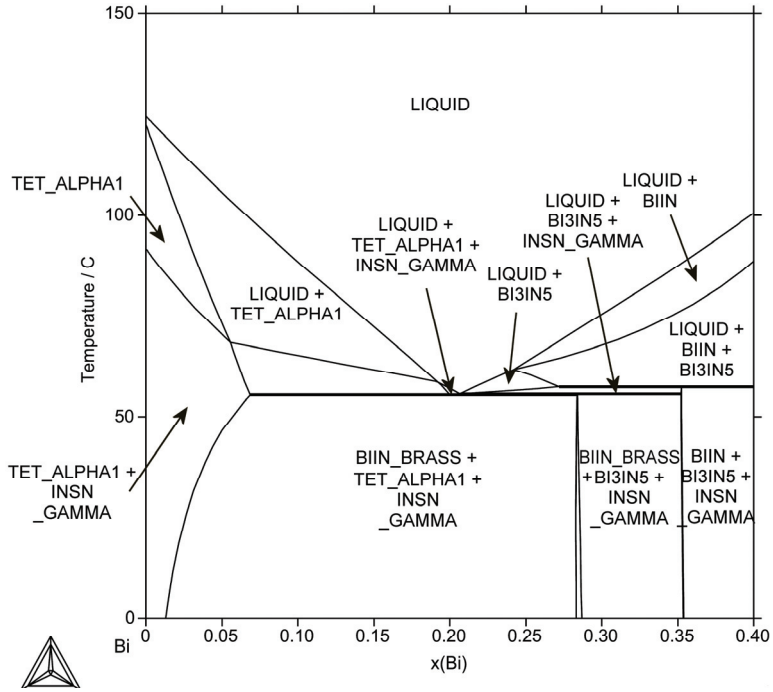

Fig. 172: Isopleth for 60 at% In (near the invariant points E1, U6)

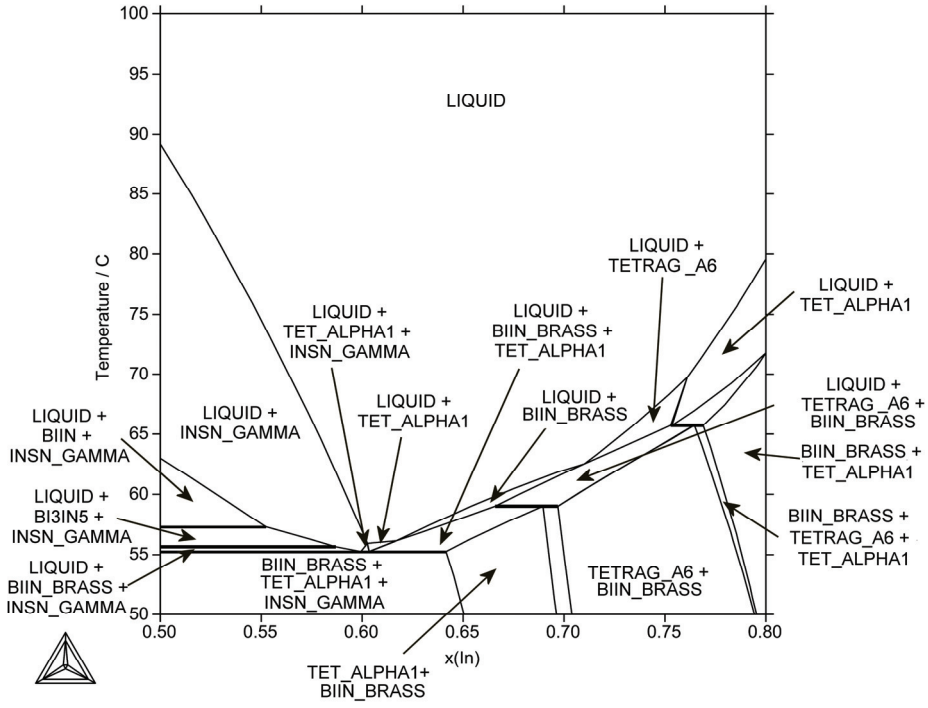

Fig. 173: Partial isopleth of the Bi-In-Sn system for 20 at% Bi

Bi-Sb-Sn System

Although Ohtani and Ishida **[94Oht]** optimized thermodynamic parameters in this ternary system, a critical evaluation of the literature data in the frame of the COST 531 program as well as new experimental thermodynamic results **[01Vas, 05Kat]** created a need for reassessment of data for the Bi-Sb-Sn system. The results of the modelling of phase equilibria are compared with experimental results from **[07Man]** and from other literature sources. Also, experimentally obtained activities and experimentally based excess Gibbs energy functions from the literature **[01Vas, 05Kat]** were used for the optimization of the thermodynamic parameters.

References:

[94Oht] Ohtani, H., Ishida, K.: *J. Electron. Mater*., 1994, **23**, 747-755.

[01Vas] Vassilev, V., Feutelais, Y., Sghaier, M., Legendre, B.: *J. Alloys Comp*., 2001, **314**, 198-205.

[05Kat] Katayama, I., Živković, D., Manasijević, D., Tanaka, T.,. Živković, Ž., Yamashita, H.: *Netsu Sokutei*, 2005, **32**, 40-44.

[07Man] Manasievič, D., Vřešťál, J., Minič, D., Kroupa, A., Živkovič, D., Živkovič, Ž.: *J. Alloys Comp.*, 2007, **438**, 150-157.

Table of invariant reactions

T / °C	Reaction type	Phases	Compositions		
			x_{Bi}	x_{Sb}	x_{Sn}
244.1	U1	LIQUID	0.004	0.088	0.908
		SB2SN3	0.000	0.400	0.600
		SBSN	0.001	0.455	0.544
		BCT_A5	0.000	0.106	0.894
138.5	U2	LIQUID	0.376	0.011	0.613
		SBSN	0.067	0.397	0.536
		RHOMBO_A7	0.954	0.014	0.032
		BCT_A5	0.064	0.011	0.925

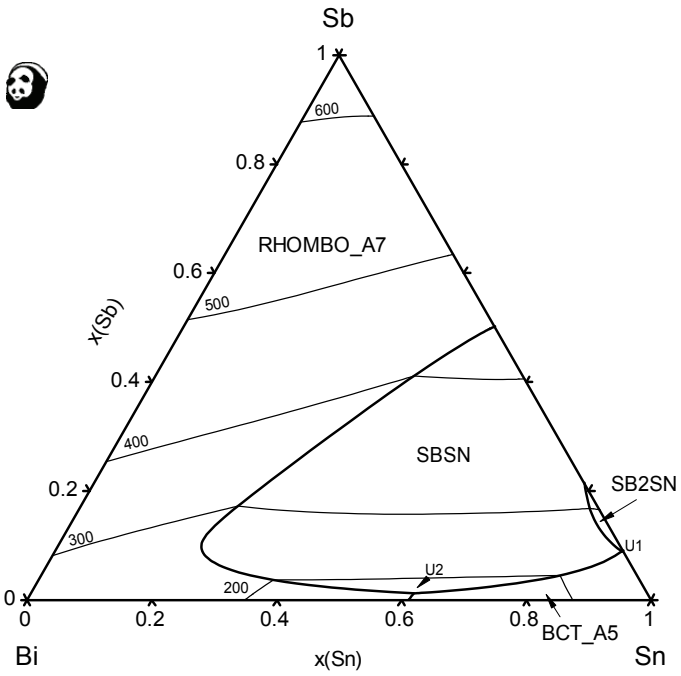

Fig. 174: Liquidus projection of the Bi-Sb-Sn system

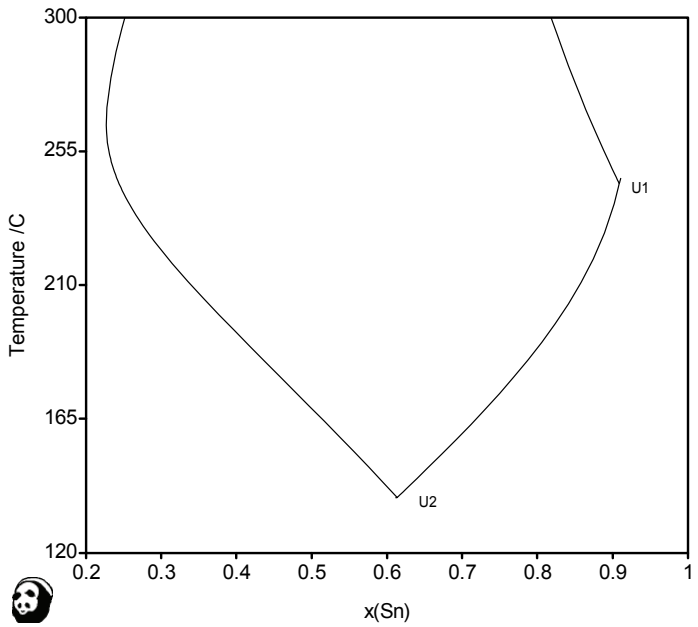

Fig. 175: Liquidus lines in the Bi-Sb-Sn system in the region of the low-temperature invariants projected onto the T- x(Sn) plane

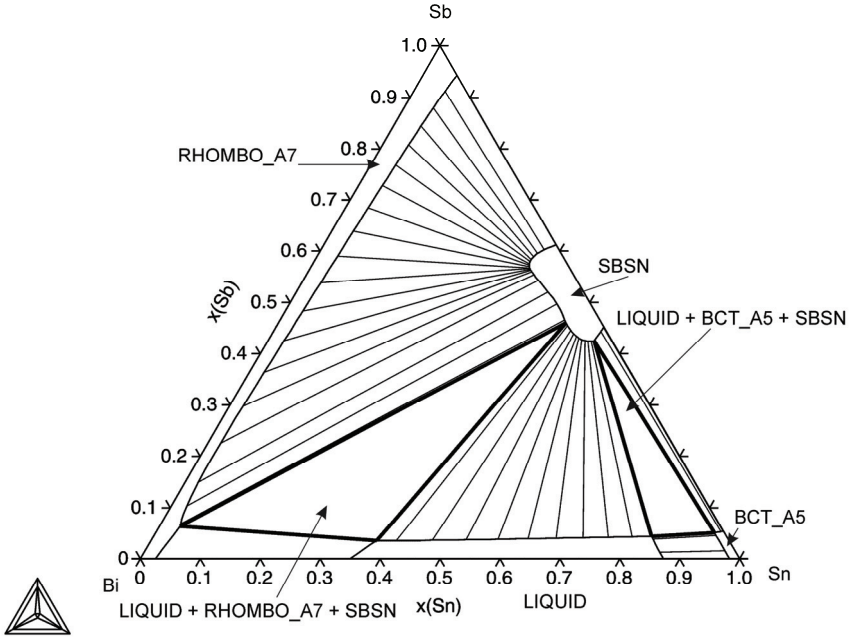

Fig. 176: Isothermal section at 200 °C

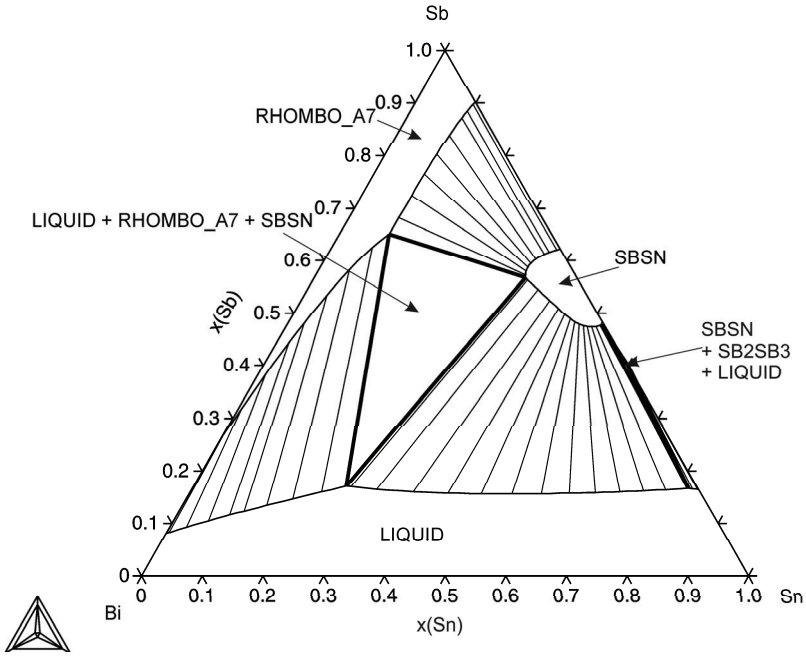

Fig. 177: Isothermal section at 300 °C

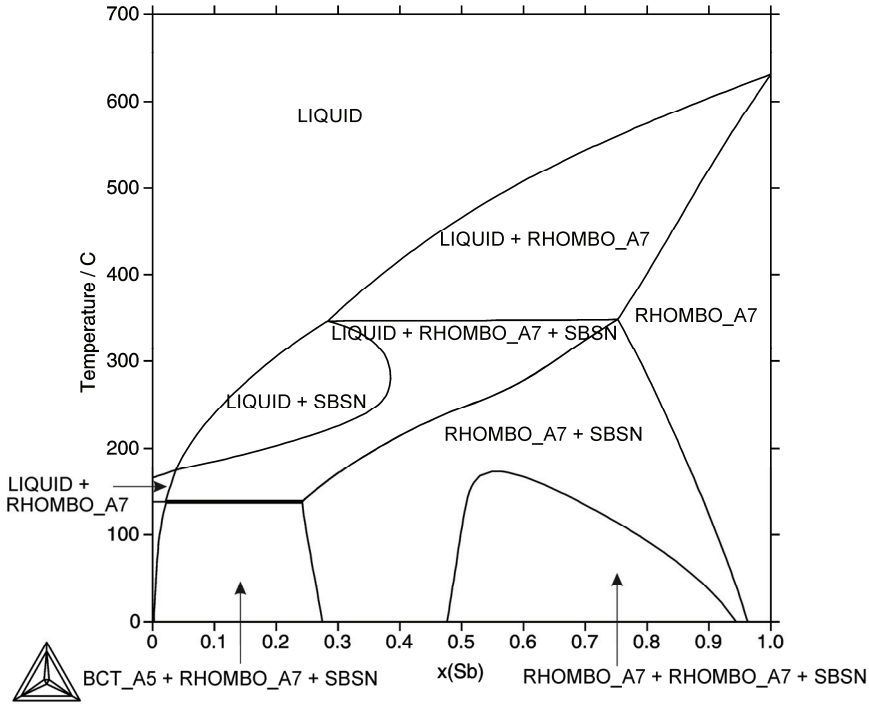

Fig. 178: Isopleth of the Bi-Sb-Sn system with the ratio Bi:Sn of 1:1

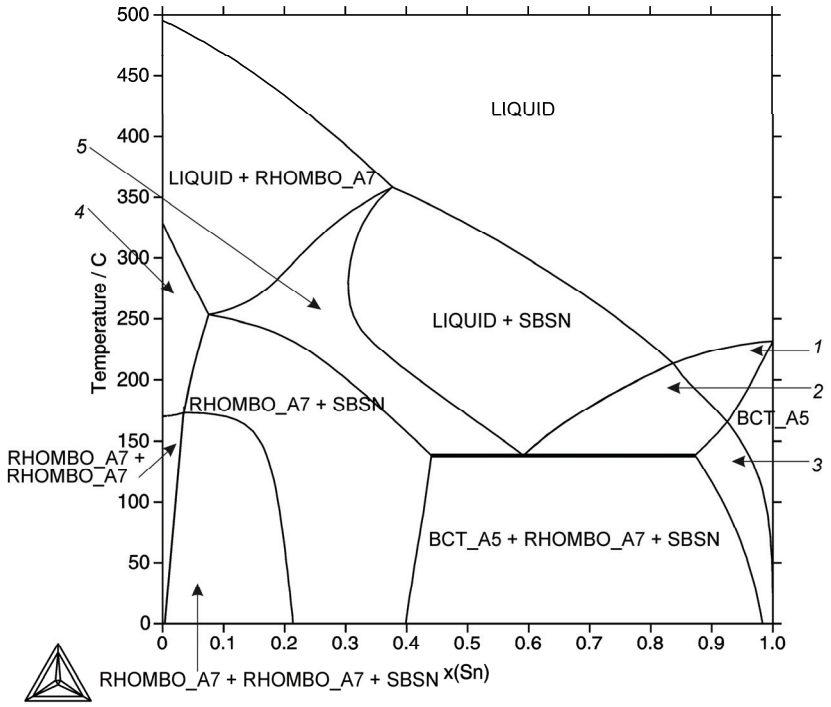

Fig. 179: Isopleth of the Bi-Sb-Sn system with the ratio Bi:Sb of 1:1

Legend:

1 – BCT_A5 + LIQUID
2 – BCT_A5 + LIQUID + SBSN
3 – BCT_A5 + SBSN
4 – RHOMBO_A7
5 – LIQUID + RHOMBO_A7 + SBSN

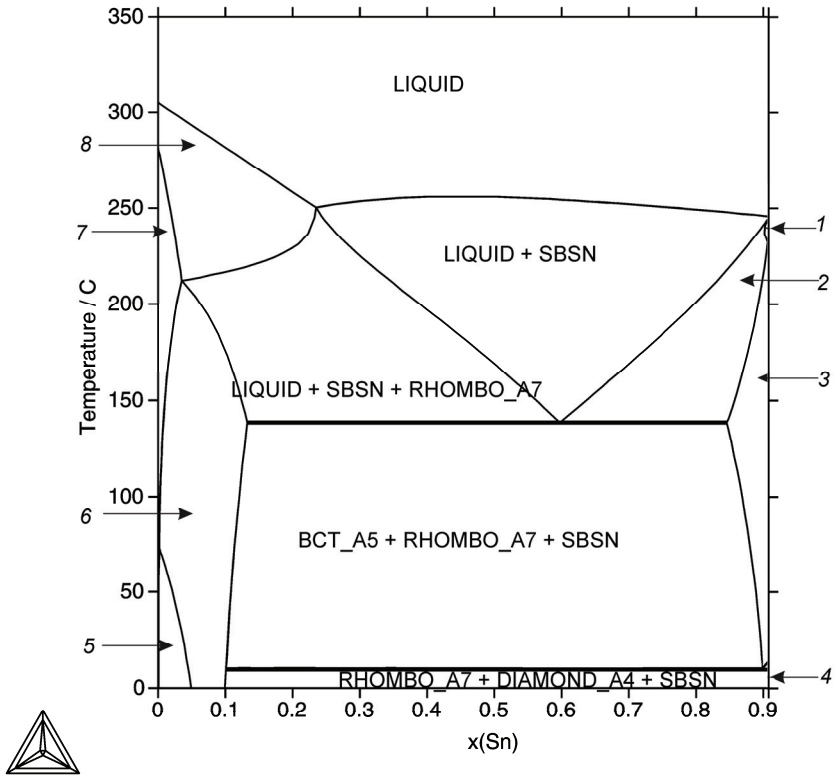

Fig. 180: Isopleth of the Bi-Sb-Sn system for 9 at% Sb

Legend:

1 – BCT_A5 + LIQUID
2 – BCT_A5 + LIQUID + SBSN
3 – BCT_A5 + SBSN
4 – DIAMOND_A4 + SBSN
5 – RHOMBO_A7 + RHOMBO_A7 + SBSN
6 – RHOMBO_A7 + SBSN
7 – RHOMBO_A7
8 – LIQUID + RHOMBO_A7

Bi-Sn-Zn System

The ternary Bi-Sn-Zn system was assessed by Malakhov *et al.* **[00Mal]** and Moelans *et al.* **[03Moe]**. Both assessments are based on the experimental work of Muzaffar **[23Muz]** and both authors introduced ternary corrections for the liquid phase only. The assessments of this system are unfortunately not mutually consistent, as the authors used different unary data and also binary data for Bi-Sn systems (**[94Oht], [96Lee]**). As both Malakhov *et al.* **[00Mal]** and Moelans *et al.* **[03Moe]** have used the older thermodynamic description of the Bi-Sn system for their assessments, it was necessary to reassess the Bi-Sn-Zn system using the newly assessed Bi-Sn system **[07Viz]**. Recently, Luef *et al.* **[06Lue]** published experimentally measured enthalpies of liquid and DSC data in Sn-rich part of the system. Braga *et al.* **[07Bra]** published new significant experimental results focusing on the miscibility gap and also the Sn-rich part of the phase diagram. These data were also utilized for the reassessment of the ternary system **[07Viz]**.

References:

[23Muz] Muzaffar, S. D.: *J. Chem. Soc.*, 1923, **123**, 2341.

[94Oht] Ohtani, H., Ishida, K.: *J. Electron. Mater.*, 1994, **23**, 747-755.

[96Lee] Lee, B.-J., Oh, C.-S., Shim, J.-H.: *J. Electron Mater.*, 1996, **25**, 983-991.

[00Mal] Malakhov, D. V., Liu, X. J., Ohnuma, I., Ishida, K.: *J. Ph. Equil.*, 2000, **21**, 514-520.

[03Moe] Moelans, N., Kumar, K. C. H., Wollants, P.: *J. All. Comp.*, 2003, **360**, 98-106.

[06Lue] Luef, C., Paul, A., Vízdal, J., Kroupa, A., Kodentsov, A. Ipser, H.: *Monatsh. Chem.*, 2006, **137**, 381-395.

[07Bra] Braga, M. H., Vízdal, J., Kroupa, A., Ferreira, J., Soares, D., Malheiros, L. F.,: *CALPHAD,* 2007, **31**, 468-478.

[07Viz] Vízdal, J., Braga, M. H., Kroupa, A., Richter, K. W., Soares, D., Malheiros, L. F., Ferreira, J.: *CALPHAD*, 2007, **31**, 438-448.

Table of invariant reactions

T / °C	Reaction type	Phases	Compositions		
			x_{Bi}	x_{Sn}	x_{Zn}
131.7	E1	LIQUID	0.355	0.601	0.044
		HCP_ZN	0.001	0.001	0.998
		RHOMBO_A7	0.973	0.026	0.001
		BCT_A5	0.060	0.936	0.004

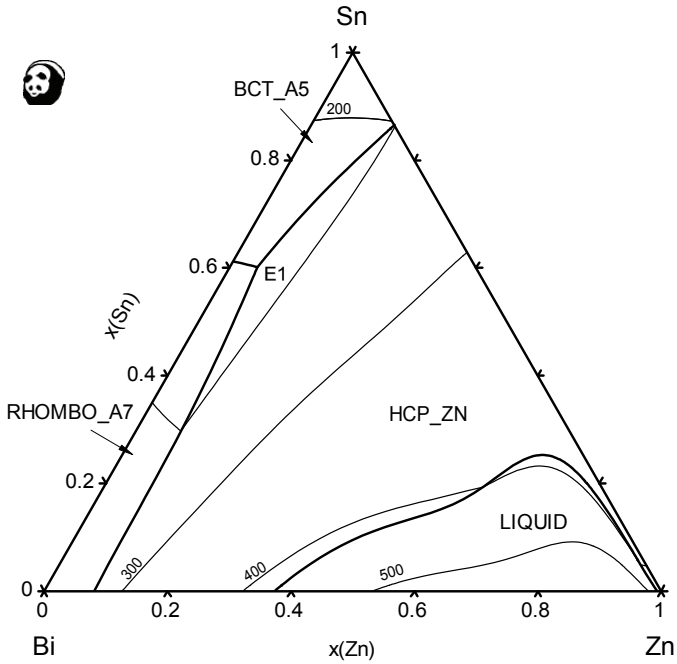

Fig. 181: Liquidus projection of the Bi-Sn-Zn system

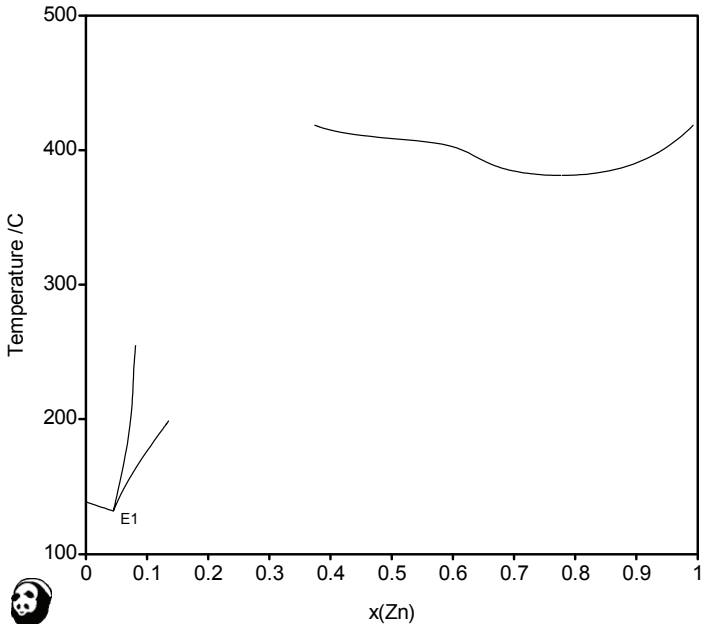

Fig. 182: Liquidus lines in the Bi-Sn-Zn system in the region of the low-temperature invariants projected onto the T- x(Zn) plane

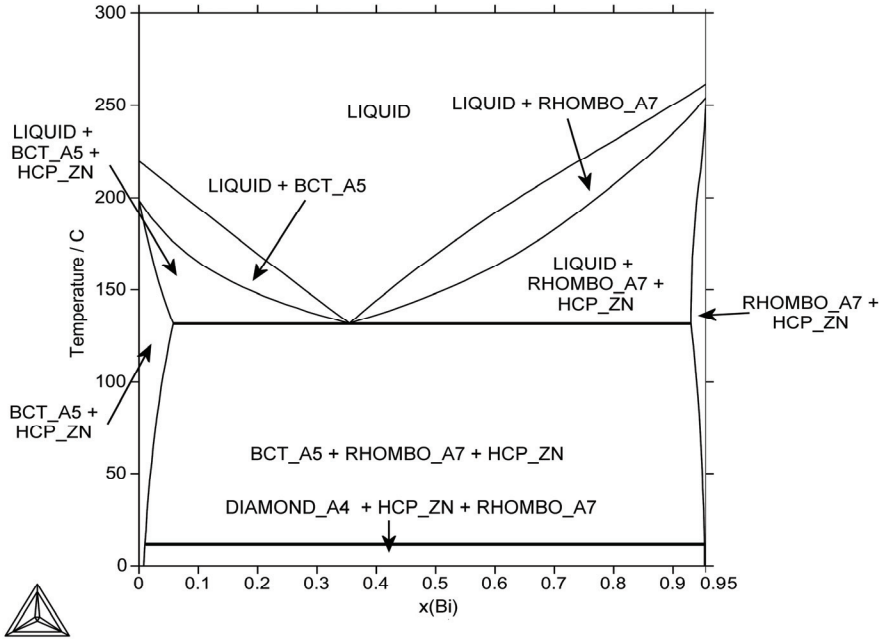

Fig. 183: Isopleth of the Bi-Sn-Zn system for 4.456 at% Zn (eutectic Zn concentration)

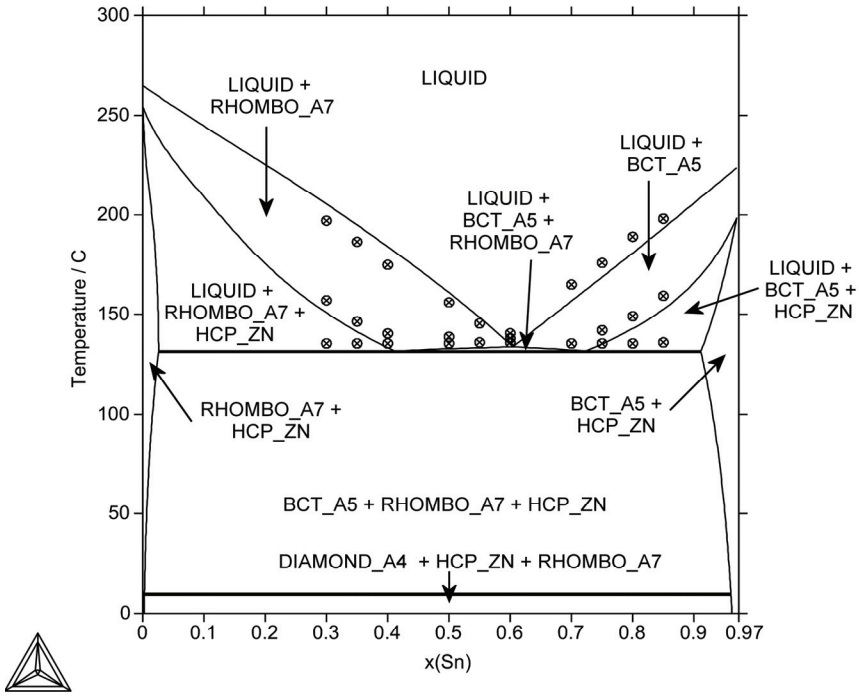

Fig. 184: Isopleth of the Bi-Sn-Zn system for 3 at% Zn (compared with exp. data from **[06Lue]**)

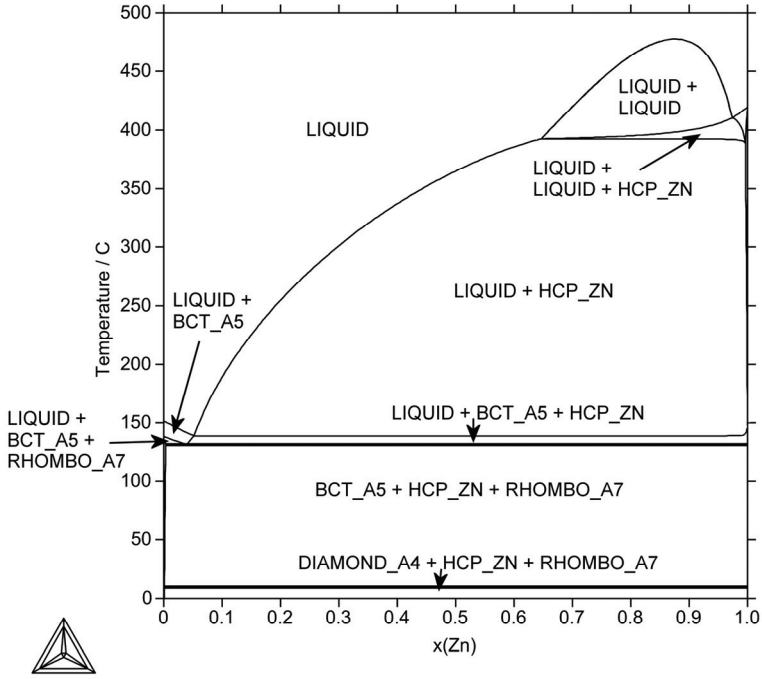

Fig. 185: Isopleth of the Bi-Sn-Zn system with the ratio Bi:Sn of 1:2

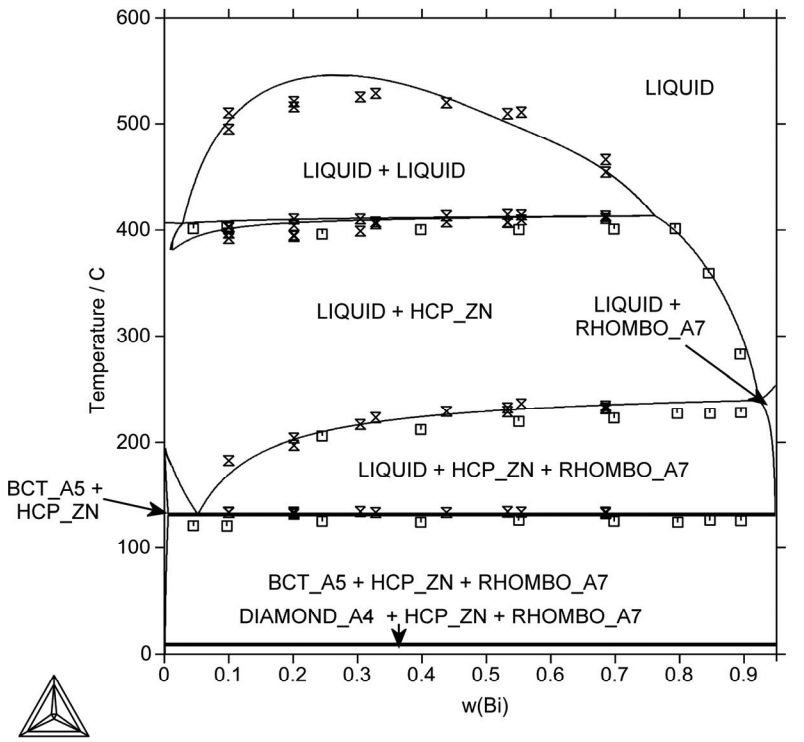

Fig. 186: Isopleth of the Bi-Sn-Zn system for 5 wt. % Sn (compared with exp. data from **[23Muz] -** ❑ and **[07Bra] -** ⧖)

Cu-In-Sn System

The data from Liu *et al.* **[01Liu]** were modified and incorporated into the database. This reassessment is based on new phase equilibrium data from **[07Dra1, 07Dra2]**, and new thermodynamic data from **[06Pop, 06Li]**.

References:

[01Liu] Liu, X. J., Liu, H. S., Ohnuma, I., Kainuma, R., Ishida, K., Itabashi, S., Kameda, K., Yamaguchi, K.: *J. Electron. Mater.*, 2001, **30**(9) 1093.

[06Pop] Popovič, A., Bencze, L.: *Int. J. of Mass Spectrometry*, 2006, **257**, 41-49.

[06Li] Li, Z., Knott, S., Qiao, Z., Mikula, A.: *Mater. Trans. A*, 2006, **47**(8), 2025-2032.

[07Dra1] Drápala, J., Burkovič, R., Kozelková, R, Smetana, B., Dočekalová, S., Dudek, R., Zlatohlávek, P., Vřešťál, J., Kroupa, A.: *Acta Metallurgica Slovaca*, 2007, **13**(1), 670-673.

[07Dra2] Drápala, J., Kubíček, P., Vřešťál, J., Losertová, M.: *Defect and Diffusion Forum,* Trans. Tech. Publication, Switzerland, 2007, **263**, 231-236.

Table of invariant reactions

T / °C	Reaction type	Phases	Compositions		
			x_{Cu}	x_{In}	x_{Sn}
667.0	U1	LIQUID	0.671	0.195	0.134
		CUIN_GAMMA	0.695	0.240	0.065
		BCC_A2	0.738	0.147	0.115
		CUIN_ETA	0.655	0.249	0.096
519.3	E1	BCC_A2	0.650	0.015	0.335
		LIQUID	0.328	0.051	0.621
		CUIN_ETA	0.585	0.089	0.326
		CU3SN	0.750	0.000	0.250
217.9	U2	LIQUID	0.011	0.060	0.929
		BCT_A5	0.000	0.021	0.979
		CUIN_ETA	0.570	0.136	0.294
		INSN_GAMMA	0.000	0.036	0.964

153.8	E2	LIQUID	0.006	0.994	0.000
		TETRAG_A6	0.000	1.000	0.000
		CUIN_ETA	0.607	0.351	0.042
		CUIN_THETA	0.550	0.450	0.000
143.6	U3	LIQUID	0.007	0.900	0.093
		CUIN_ETA	0.580	0.282	0.138
		CU2IN3SN	0.333	0.500	0.167
		TETRAG_A6	0.000	0.929	0.071
135.3	U4	LIQUID	0.010	0.833	0.157
		TETRAG_A6	0.000	0.876	0.124
		CU2IN3SN	0.333	0.500	0.167
		TET_ALPHA1	0.000	0.868	0.132
109.1	U5	LIQUID	0.014	0.542	0.444
		CU2IN3SN	0.333	0.500	0.167
		CUIN_ETA	0.573	0.233	0.194
		TET_ALPHA1	0.000	0.572	0.428
109.0	E3	LIQUID	0.013	0.540	0.447
		CUIN_ETA	0.573	0.233	0.194
		TET_ALPHA1	0.000	0.570	0.430
		INSN_GAMMA	0.000	0.229	0.771

Phase information

Phase Name	Common Name	Strukturbericht designation/type	Pearson Symbol
CU2IN3SN	Cu_2In_3Sn	...	...
CU77INSN23	$Cu_{77}(In,Sn)_{23}$	...	...

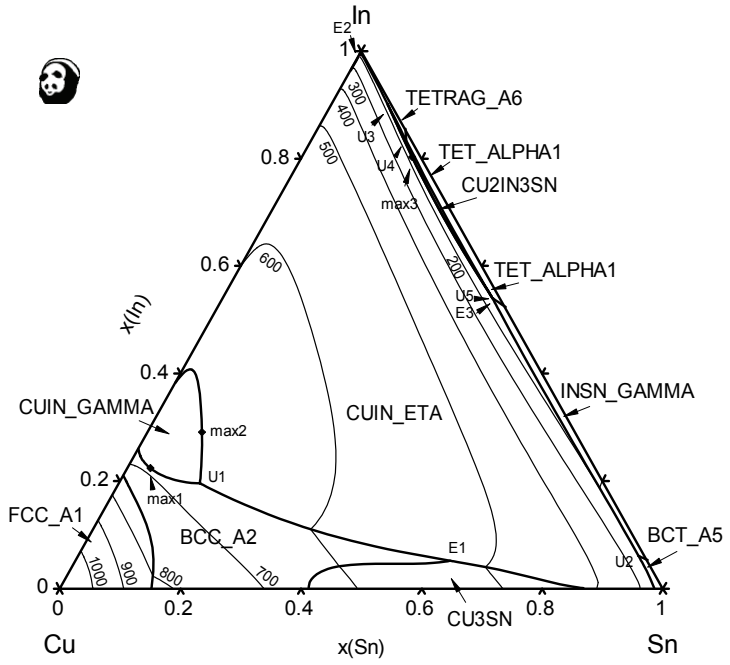

Fig. 187: Liquidus projection of the Cu-In-Sn system

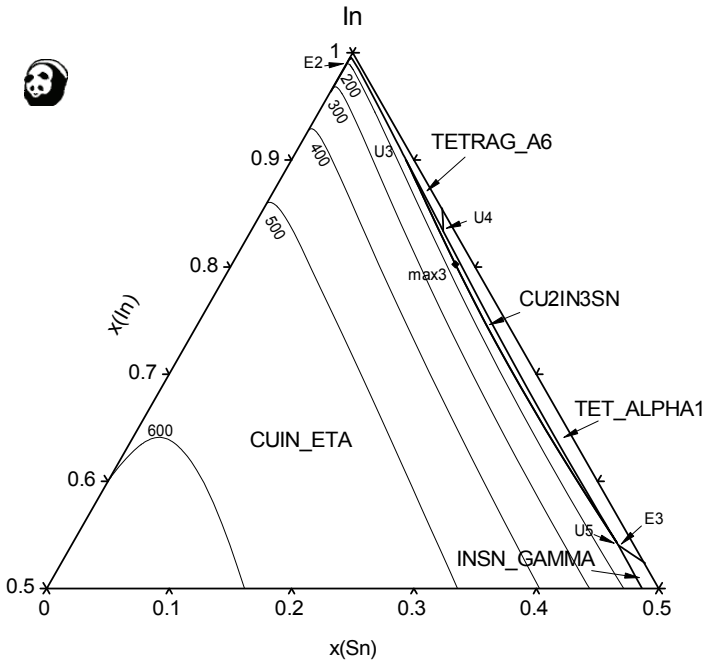

Fig. 188: Liquidus projection for the In rich corner of the Cu-In-Sn system

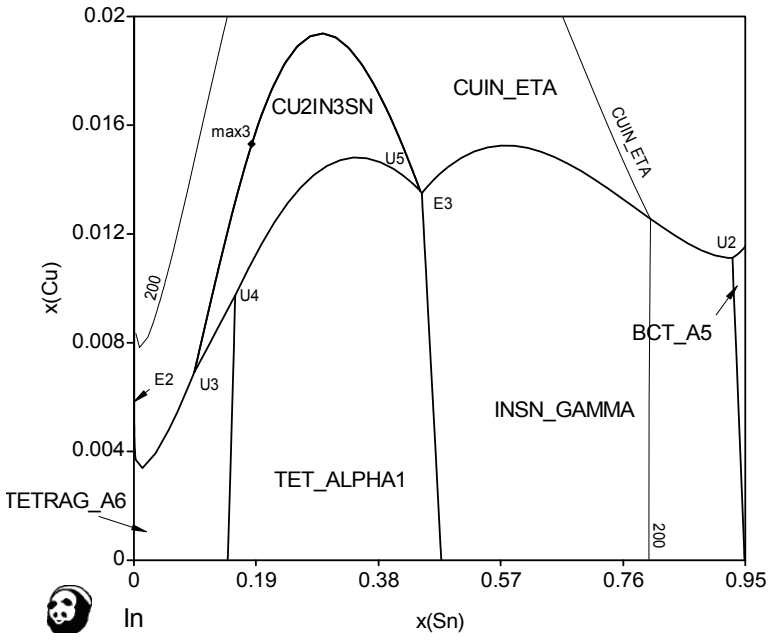

Fig. 189: Liquidus lines in the region close to the In-Sn binary edge in the Cu-In-Sn system

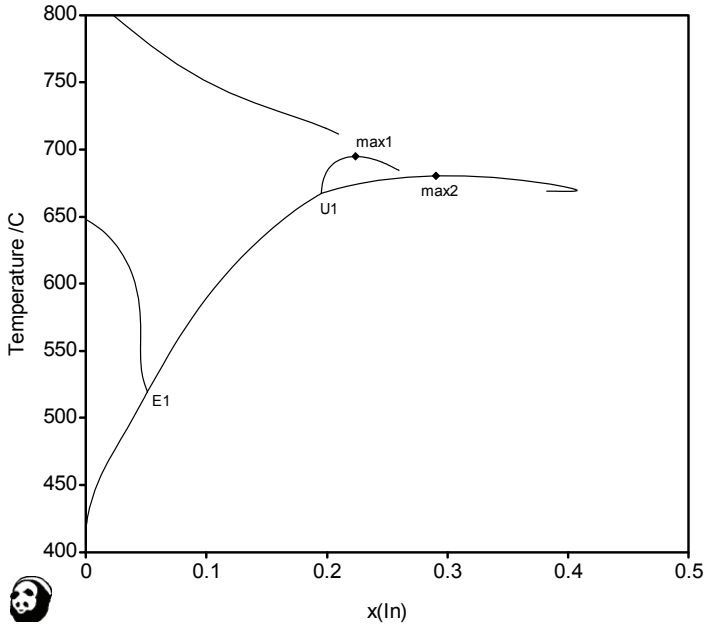

Fig. 190: Liquidus lines in the Cu-In-Sn system in the region of the high-temperature invariants projected onto the T- x(In) plane

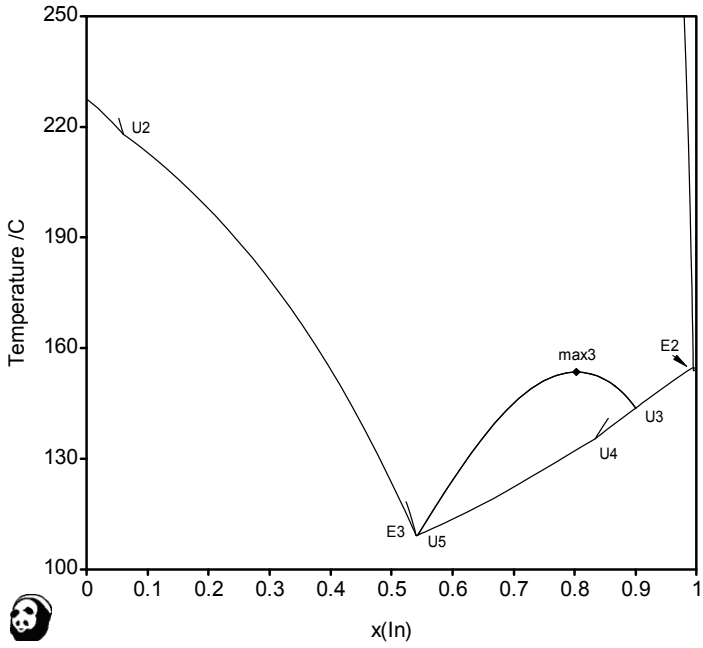

Fig. 191: Liquidus lines in the Cu-In-Sn system in the region of the low-temperature invariants projected onto the T- x(In) plane

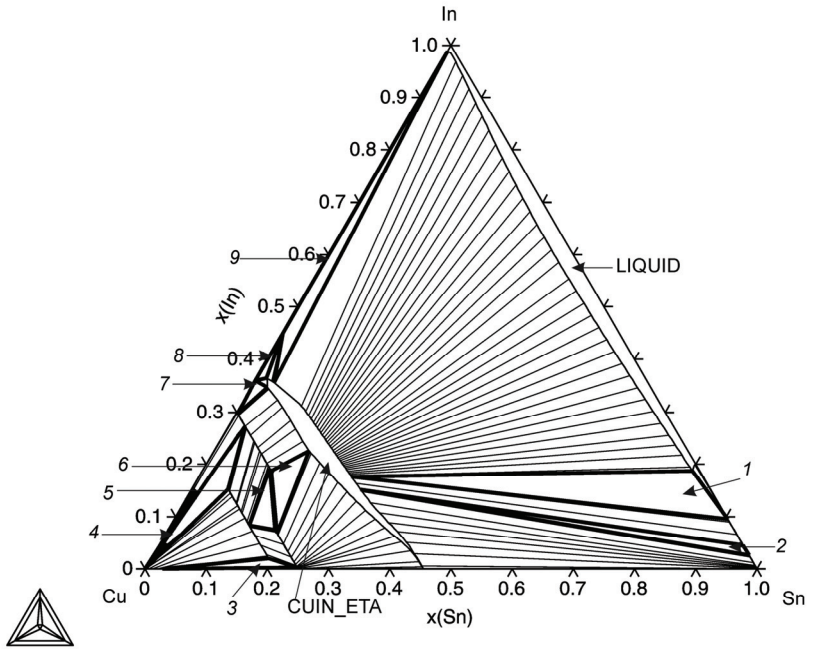

Fig. 192: Isothermal section at 200 °C

Legend:

1 – LIQUID + CUIN_ETA + INSN_GAMMA
2 – CUIN_ETA + INSN_GAMMA + BCT_A5
3 – FCC_A1 + CU41SN11 + CU3SN
4 – FCC_A1 + CU41SN11 + CUIN_DELTA
5 – CU41SN11 + CUIN_DELTA + CU3SN
6 – CUIN_DELTA + CU3SN + CUIN_ETA
7 – CUIN_DELTA + CUIN_ETA + CUIN_ETAP
8 – CUIN_ETA + CUIN_ETAP + CUIN_THETA
9 – LIQUID + CUIN_THETA + CUIN_ETA

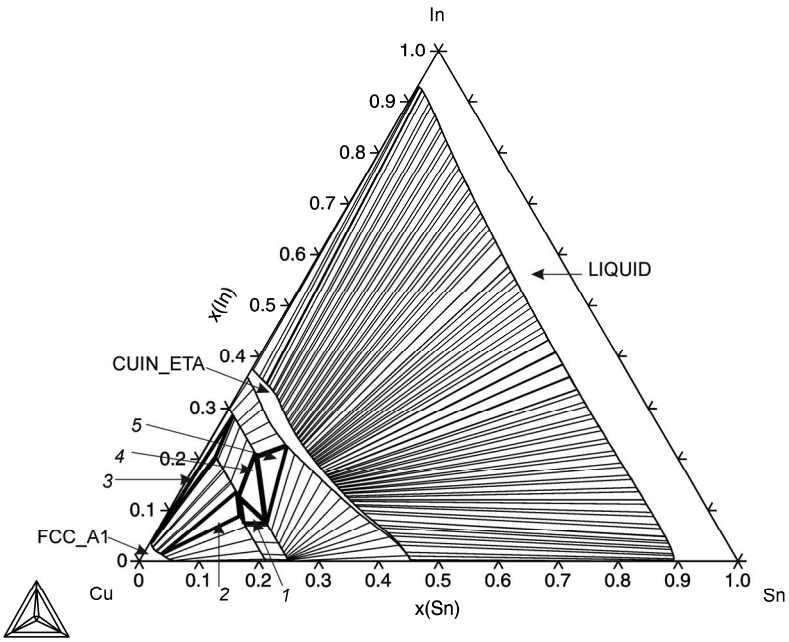

Fig. 193: Isothermal section at 400 °C

Legend:

1 – CU41SN11 + CU77INSN23 + CU3SN
2 – CU41SN11 + CU77INSN23 + FCC_A1
3 – CU77INSN23 + CUIN_DELTA + FCC_A1
4 – CU77INSN23 + CUIN_DELTA + CU3SN
5 – CUIN_DELTA + CUIN_ETA + CU3SN

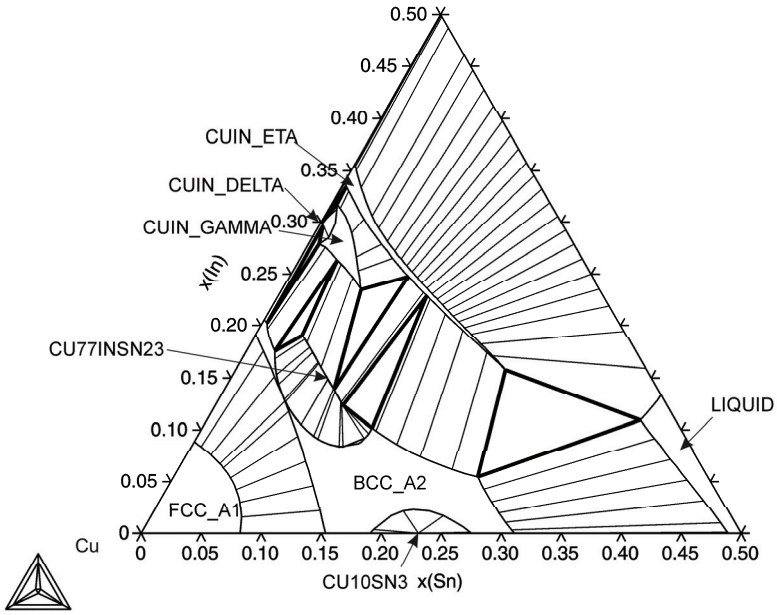

Fig. 194: Cu-rich corner of the isothermal section at 600 °C

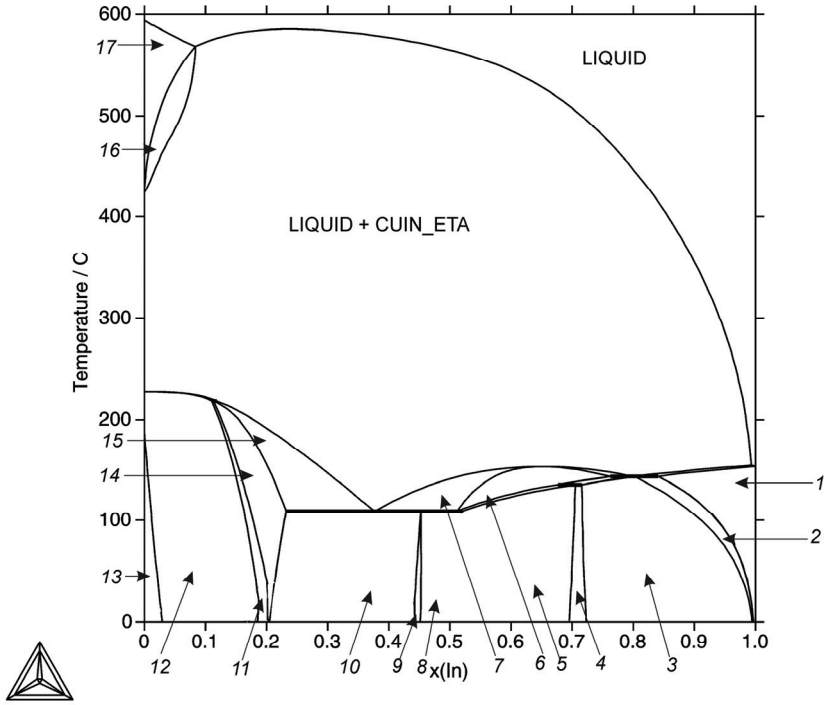

Fig. 195: Isopleth of the Cu-In-Sn system with the ratio Cu:Sn of 1:1

Legend:

1 – CU2IN3SN + TET_ALPHA1
2 – CUIN_ETA + TETRAG_A6
3 – CU2IN3SN + TETRAG_A6
4 – CU2IN3SN + TETRAG_A6 + TET_ALPHA1
5 – CU2IN3SN + TET_ALPHA1
6 – LIQUID + CU2IN3SN
7 – LIQUID + CUIN_ETA + CU2IN3SN
8 – CU2IN3SN + INSN_GAMMA + TET_ALPHA1
9 – CU2IN3SN + INSN_GAMMA
10 – CUIN_ETA + CU2IN3SN + INSN_GAMMA
11 – CUIN_ETA + BCT_A5 + INSN_GAMMA
12 – CUIN_ETA + BCT_A5 + CU6SN5_P
13 – CUIN_ETA + BCT_A5
14 – CUIN_ETA + INSN_GAMMA
15 – CUIN_ETA + INSN_GAMMA+ LIQUID
16 – CUIN_ETA + CU3SN + LIQUID
17 – CU3SN + LIQUID

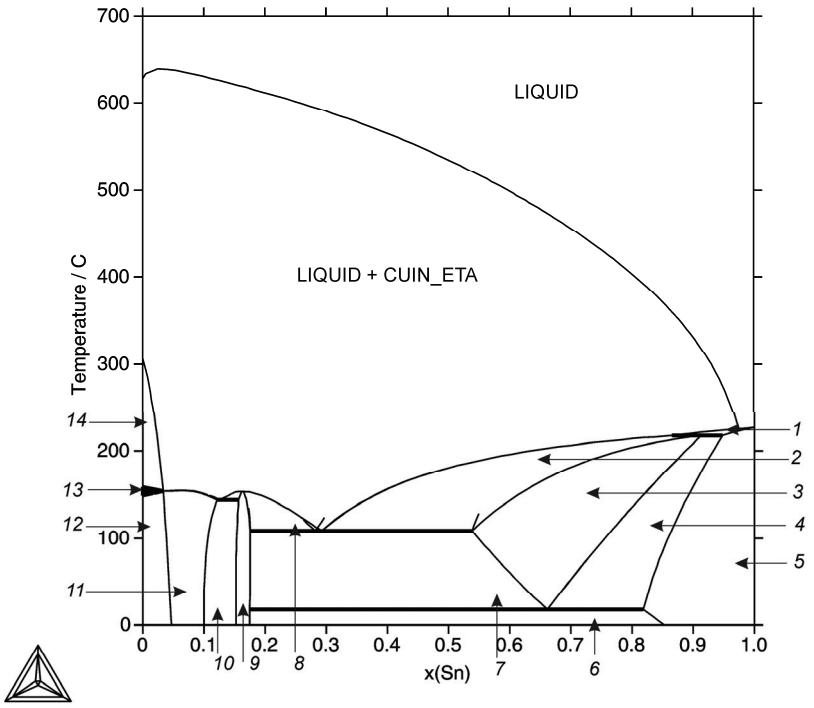

Fig. 196: Isopleth of the Cu-In-Sn system with the ratio Cu:In of 1:1

Legend:

1 – LIQUID + CUIN_ETA + BCT_A5
2 – LIQUID + CUIN_ETA + INSN_GAMMA
3 – CUIN_ETA + INSN_GAMMA
4 – CUIN_ETA + INSN_GAMMA + BCT_A5
5 – CUIN-ETA + BCT_A5
6 – CUIN-ETA + CU2IN3SN + DIAMOND_A4
7 – CUIN_ETA + CU2IN3SN + INSN_GAMMA
8 – CUIN_THETA + CUIN_ETA + TETRAG_A6
9 – CUIN_ETA + CU2IN3SN
10 – CUIN_ETA + CU2IN3SN + TETRAG_A6
11 – CUIN_ETA + CUIN_THETA + LIQUID
12 – CUIN_ETA + CUIN_THETA + LIQUID
13 – CUIN_ETA + CU2IN3SN + LIQUID
14 – CUIN_ETA + CUIN_THETA + LIQUID

Cu-Ni-Sn System

The data for this ternary system were based on the work of Miettinen **[03Mie]**. In the assessment of **[03Mie]** different unary data and different descriptions of the relevant binary systems were used from those adopted for the COST 531 database. In addition, the high-temperature Ni_3Sn-γ phase was modelled as $D0_3$ and the ordering reaction in the Cu-Sn system was modelled in as BCC_A2→$D0_3$. Therefore, it was necessary to reassess this system to ensure compatibility with the adopted unary and binary data in the COST 531 thermodynamic database. The data for this system were derived in the scope of COST 531 Action, also using new experimental data from **[08Sch].**

References:

[03Mie] Miettinnen, J.: *CALPHAD*, 2003, **27**, 309-318.

[08Sch] Schmetterer, C., Flandorfer, H., Luef, C., Ipser H., submitted to *J. Electron. Mater.*

Table of invariant reactions

T / °C	Reaction type	Phases	Compositions		
			x_{Cu}	x_{Ni}	x_{Sn}
585.9	E1	BCC_A2	0.667	0.018	0.315
		LIQUID	0.449	0.033	0.518
		NI3SN2	0.465	0.109	0.426
		CU3SN	0.743	0.007	0.250
428.5	E2	NI3SN2	0.427	0.129	0.444
		LIQUID	0.191	0.023	0.786
		CU3SN	0.749	0.001	0.250
		NI3SN4	0.120	0.327	0.553
413.9	U1	LIQUID	0.155	0.013	0.832
		CU3SN	0.749	0.001	0.250
		NI3SN4	0.122	0.324	0.554
		CUIN_ETA	0.545	0.000	0.455
227.2	E3	LIQUID	0.015	0.000	0.985
		NI3SN4	0.146	0.301	0.553
		CUIN_ETA	0.545	0.000	0.455
		BCT_A5	0.000	0.000	1.000

Phase information

Phase Name	Common Name	Strukturbericht designation	Pearson Symbol
CU3NI27SN10	$Cu_3Ni_{27}Sn_{10}$	…	…

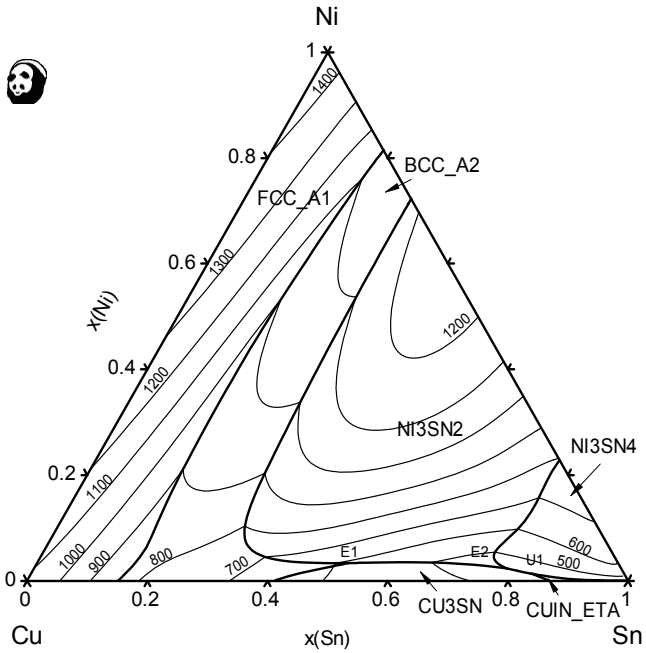

Fig. 197: Liquidus projection of the Cu-Ni-Sn system

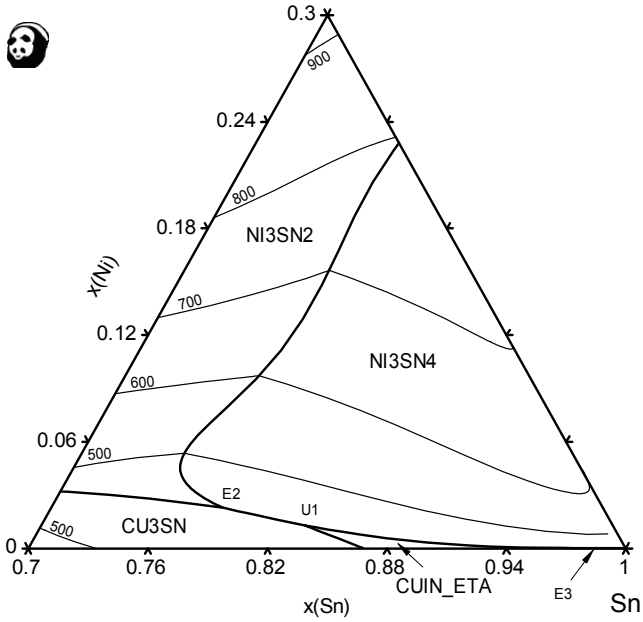

Fig. 198: Liquidus projection for the Sn rich corner of the Cu-Ni-Sn system

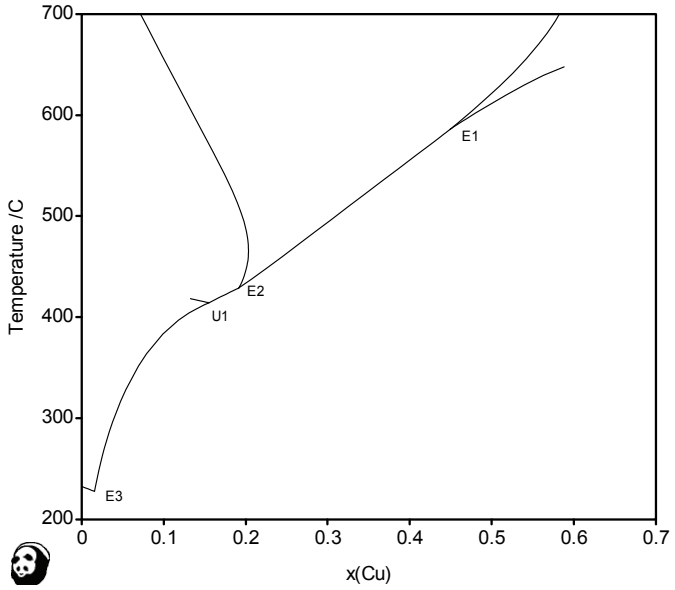

Fig. 199: Liquidus lines in the Cu-Ni-Sn system in the region of the low-temperature invariants projected onto the T- x(Cu) plane

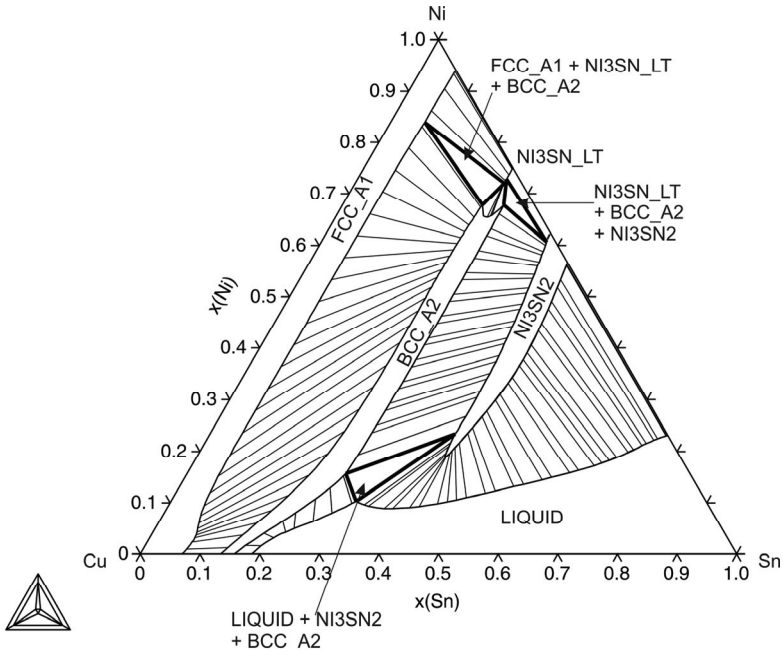

Fig. 200: Isothermal section at 800 °C

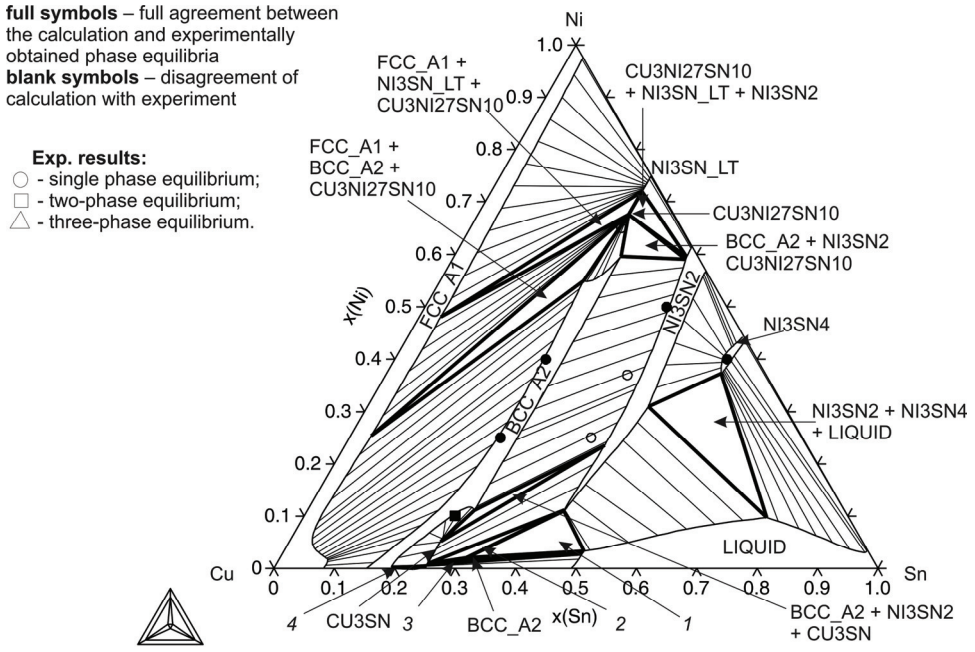

Fig. 201: Calculated isothermal section at 600 °C (compared with exp. data from **[08Sch]** obtained in the scope of COST 531 Action)

Legend:

1 – NI3SN2 + BCC_A2 + LIQUID
2 – NI3SN2 + BCC_A2 + CU3SN
3 – LIQUID + BCC_A2 + CU3SN
4 – CU10SN3 + BCC_A2 + CU3SN

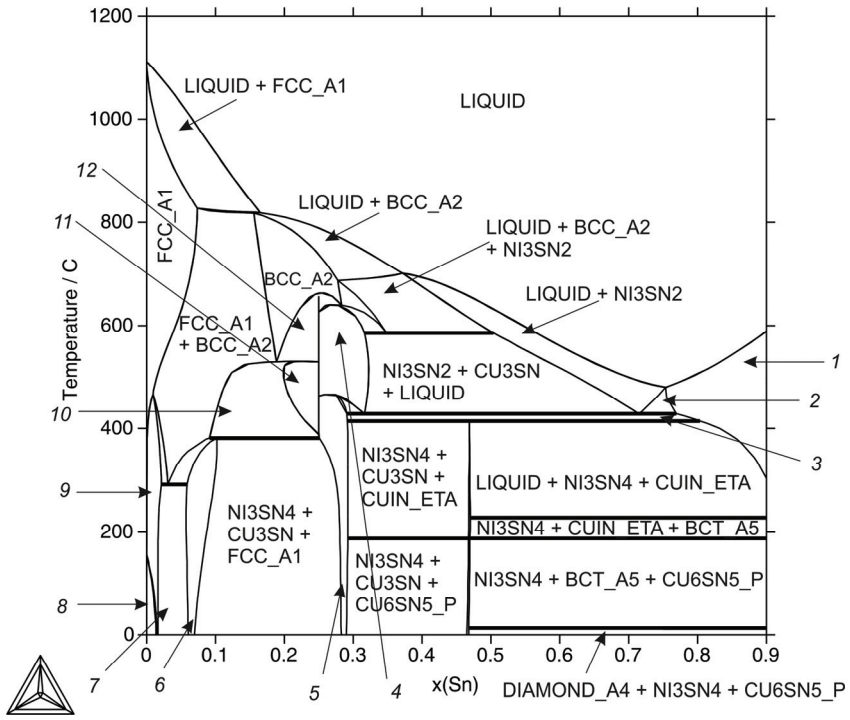

Fig. 202: Isopleth of the Cu-Ni-Sn system for 4.5 at% Ni

Legend:

1 – LIQUID + NI3SN4
2 – LIQUID + NI3SN4 + NI3SN2
3 – LIQUID + NI3SN4 + CU3SN
4 – CU3SN + NI3SN2
5 – CU3SN + NI3SN4
6 – FCC_A1 + NI3SN4
7 – FCC_A1 + CU3NI27SN10
8 – FCC_A1 + NI3SN_LT
9 – FCC_A1 + NI3SN4 + CU3NI27SN10
10 – FCC_A1 + BCC_A2 + CU3SN
11 – FCC_A1 + CU3SN
12 – CU3SN + BCC_A2

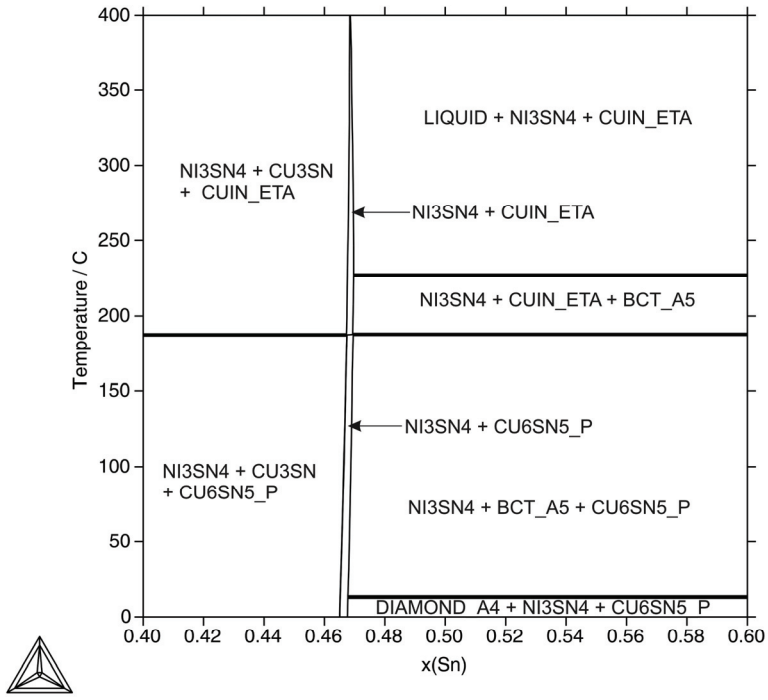

Fig. 203: Detail of the isopleths of the Cu-Ni-Sn system for 4.5 at% Ni

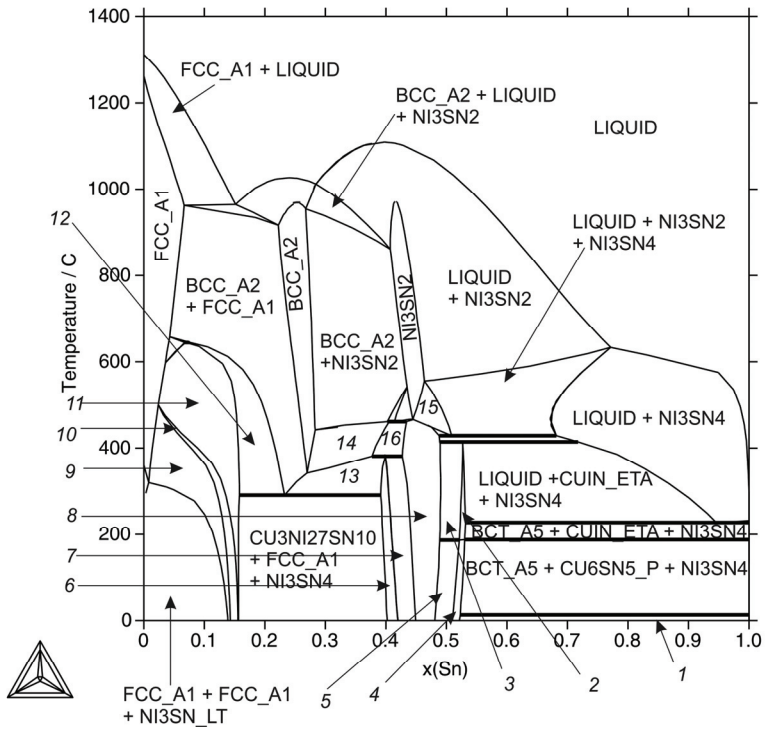

Fig. 204: Isopleth of the Cu-Ni-Sn system with the ratio Cu:Ni of 1:1

Legend:

1 – DIAMOND_A4 + NI3SN4 + CU6SN5_P
2 – CUIN_ETA + NI3SN4
3 – CUIN_ETA + NI3SN4 + CU3SN
4 – CU6SN5_P + NI3SN4
5 – CU6SN5_P + NI3SN4 + CU3SN
6 – FCC_A1 + NI3SN4
7 – FCC_A1 + NI3SN4 + CU3SN
8 – NI3SN4 + CU3SN
9 – FCC_A1 + NI3SN_LT
10 – FCC_A1 + NI3SN_LT + CU3NI27SN10
11 – FCC_A1 + CU3NI27SN10
12 – FCC_A1 + CU3NI27SN10 + BCC_A2
13 – FCC_A1 + BCC_A2 + NI3SN4
14 – BCC_A2 + NI3SN4
15 – NI3SN2 + NI3SN4
16 – BCC_A2 + CU3SN + NI3SN4

In-Sb-Sn System

Ishihara *et al.* **[99Ish]** have already provided optimized thermodynamic parameters for this ternary system. Nevertheless a critical evaluation of the literature data carried out within the framework of the COST 531 Action was necessary in view of the new thermodynamic assessment of the Sb-Sn binary system **[07Kro]** and experimental results from **[06Man].** These formed the basis for the reassessment of the data for this system by **[06Man]**. The results of thermodynamic modelling of ternary In-Sb-Sn system were compared with their own experimental results and literature data.

References:

[99Ish] Ishihara, S., Ohtani, H., Saito, T., Ishida, K.: *J. Japan Inst. Metals*, 1999, **63**(6) 695-701.

[06Man] Manasijevič, D., Vřešťál, J., Minič, D., Kroupa, A., Živkovič, D., Živkovič, Ž: *J. Alloys Compd.*, 2006, **438**, 150-157.

[07Kro] Kroupa, A., Vízdal, J.: *Defect and Diffusion Forum*, 2007, **263**, 99-104.

Table of invariant reactions

T / °C	Reaction type	Phases	Compositions		
			x_{In}	x_{Sb}	x_{Sn}
413.9	U1	LIQUID	0.127	0.507	0.366
		RHOMBO_A7	0.003	0.874	0.122
		SBSN	0.057	0.693	0.250
		ZINCBLENDE_B3	0.500	0.500	0.000
244.9	U2	LIQUID	0.002	0.090	0.908
		SB2SN3	0.000	0.400	0.600
		SBSN	0.002	0.455	0.544
		BCT_A5	0.001	0.107	0.892
234.9	U3	LIQUID	0.031	0.083	0.886
		SBSN	0.018	0.443	0.539
		ZINCBLENDE_B3	0.500	0.500	0.000
		BCT_A5	0.010	0.093	0.897

209.1	U4	LIQUID	0.120	0.014	0.866
		BCT_A5	0.042	0.012	0.946
		ZINCBLENDE_B3	0.500	0.500	0.000
		INSN_GAMMA	0.067	0.000	0.933
139.7	U5	LIQUID	0.853	0.002	0.145
		TETRAG_A6	0.876	0.000	0.124
		ZINCBLENDE_B3	0.500	0.500	0.000
		TET_ALPHA1	0.868	0.000	0.132
117.8	E1	LIQUID	0.524	0.001	0.475
		ZINCBLENDE_B3	0.500	0.500	0.000
		INSN_GAMMA	0.227	0.000	0.773
		TET_ALPHA1	0.555	0.000	0.445

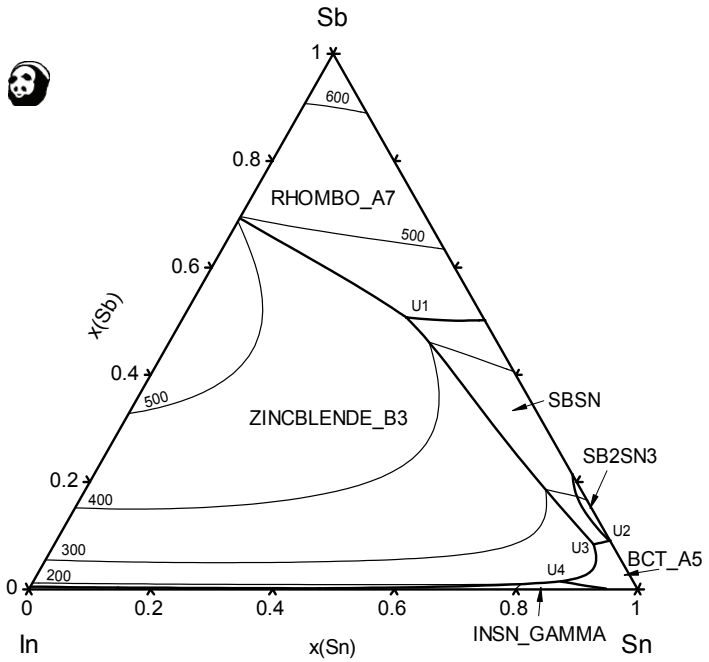

Fig. 205: Liquidus projection of the In-Sb-Sn system

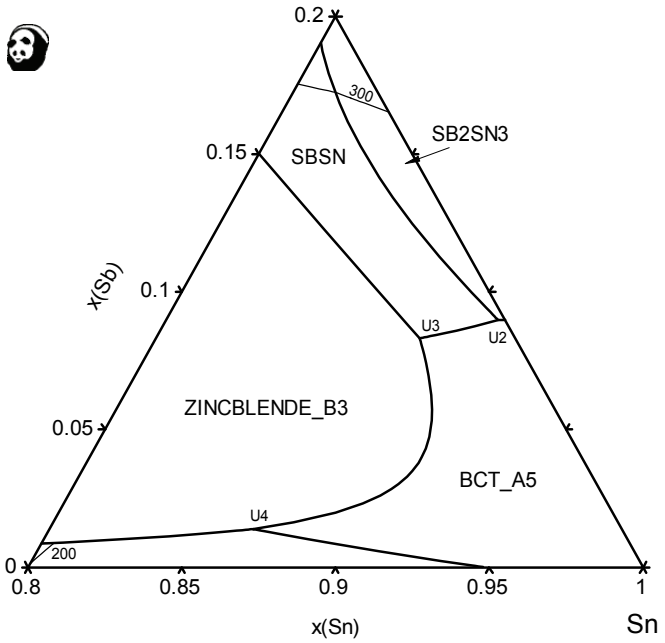

Fig. 206: Magnified view of the Sn-rich corner of the In-Sb-Sn system

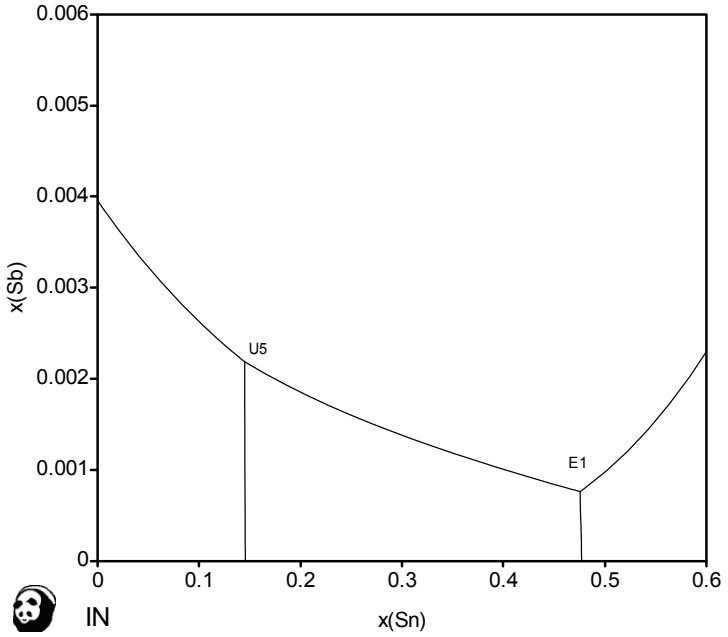

Fig. 207: Magnified view of the In- rich corner of the In-Sb-Sn system

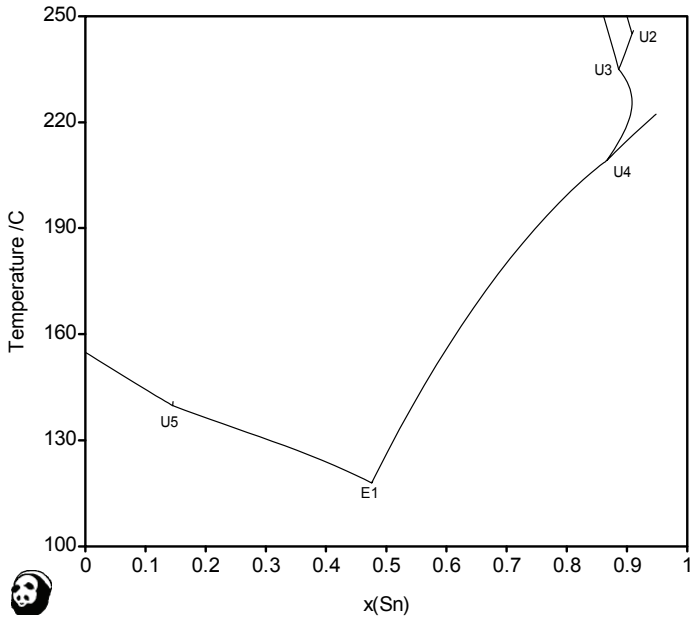

Fig. 208: Liquidus lines in the In-Sb-Sn system in the region of the low-temperature invariants projected onto the T- x(Sn) plane

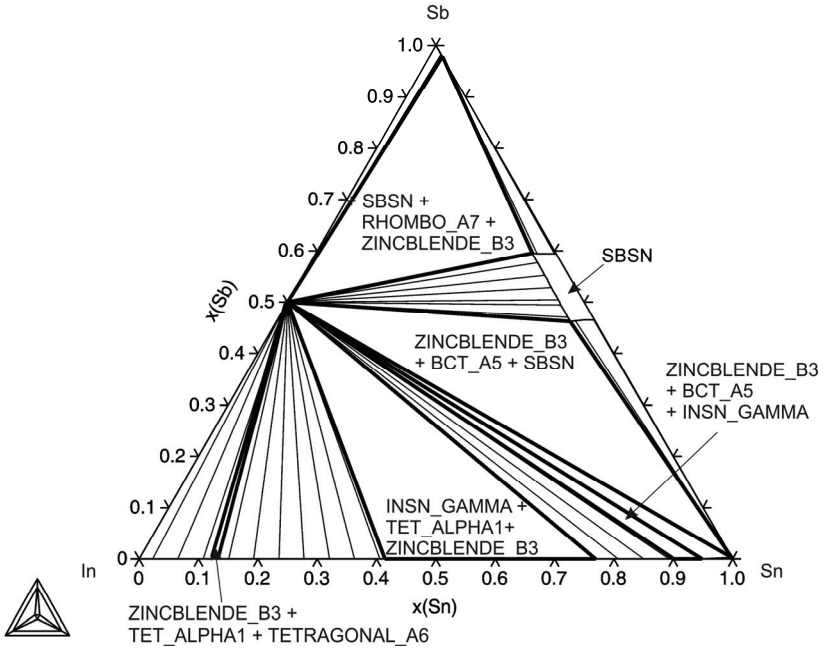

Fig. 209: Isothermal section at 100 °C

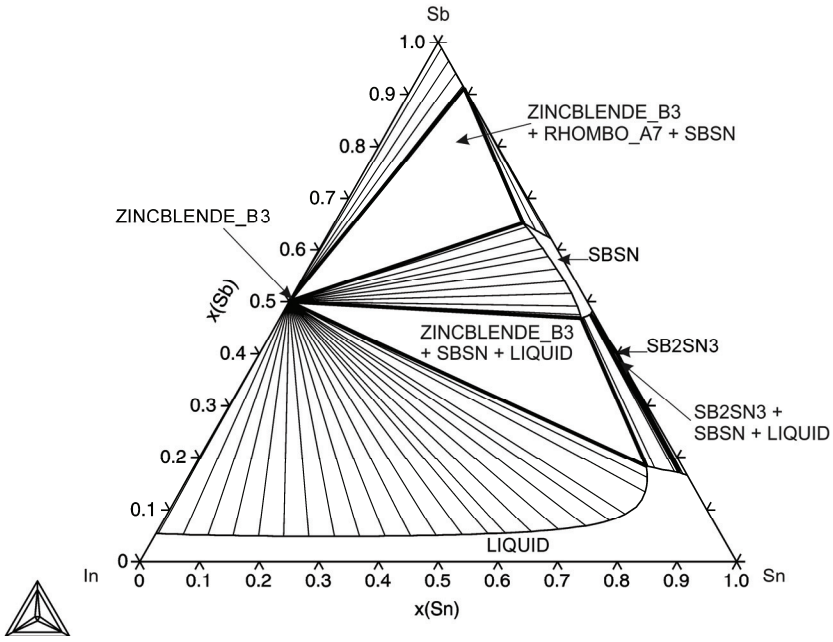

Fig. 210: Isothermal section at 300 °C

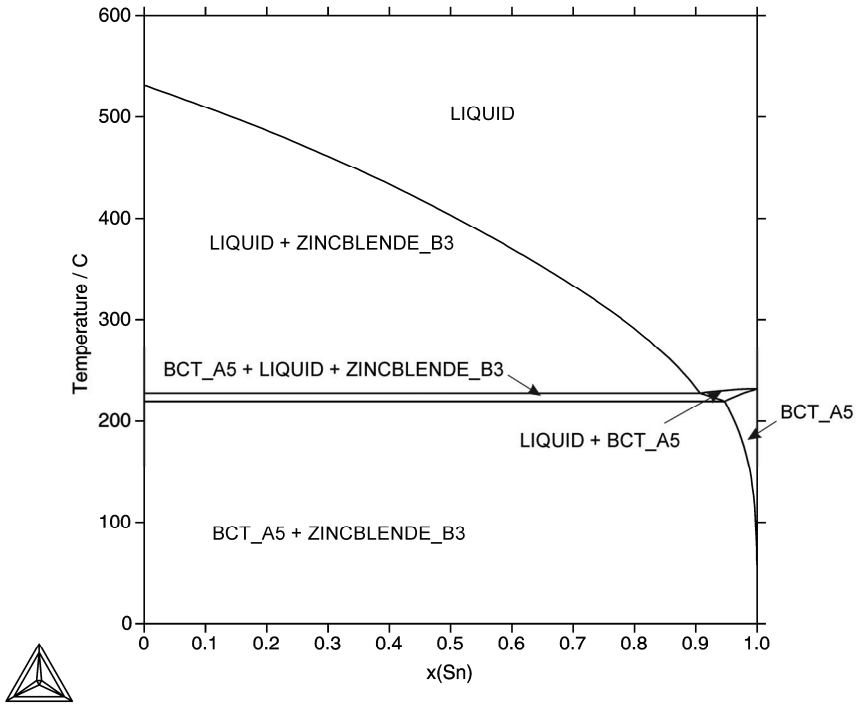

Fig. 211: Isopleth of the In-Sb-Sn system with the ratio In:Sb of 1:1

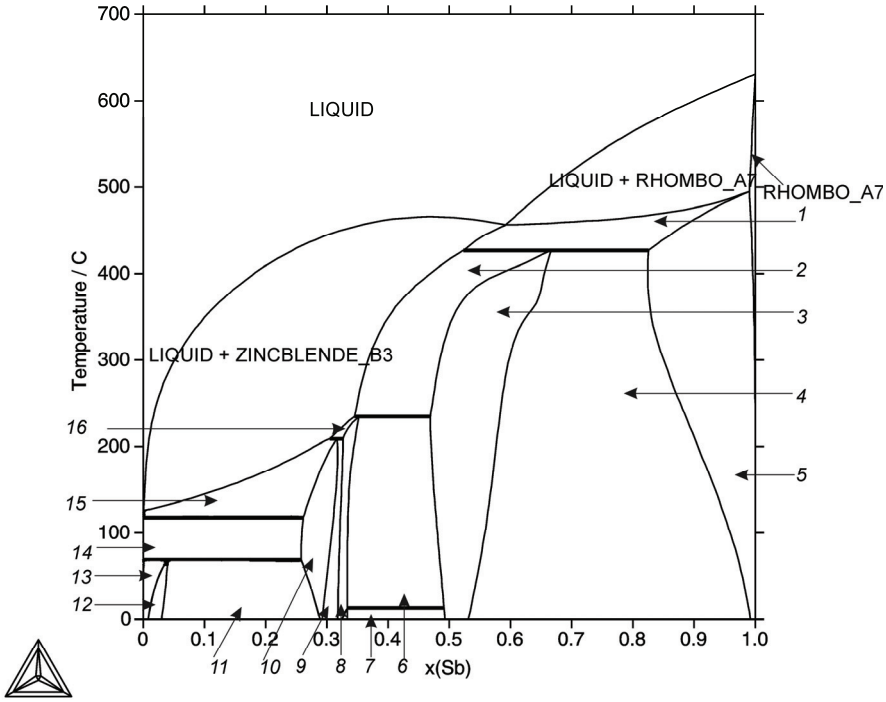

Fig. 212: Isopleth of the In-Sb-Sn system with the ratio In:Sn of 1:1

Legend:

1 – LIQUID + RHOMBO_A7 + ZINCBLENDE_B3
2 – LIQUID + ZINCBLENDE_B3 + SBDSN
3 – ZINCBLENDE_B3 + SBSN
4 – ZINCBLENDE_B3 + RHOMBO_A7 + SBSN
5 – ZINCBLENDE_B3 + RHOMBO_A7
6 – ZINCBLENDE_B3 + BCT_A5 + SBSN
7 – ZINCBLENDE_B3 + INSN_GAMMA + BCT_A5
8 – ZINCBLENDE_B3 + BCT_A5 + SBSN
9 – ZINCBLENDE_B3 + BCT_A5
10 – ZINCBLENDE_B3 + INSN_GAMMA + BCT_A5
11 – ZINCBLENDE_B3 + INSN_GAMMA + SBSN
12 – ZINCBLENDE_B3 + SBSN
13 – ZINCBLENDE_B3 + SBSN + TET_ALPHA1
14 – ZINCBLENDE_B3 + TET_ALPHA1 + INSN_GAMMA
15 – ZINCBLENDE_B3 + INSN_GAMMA + LIQUID
16 – ZINCBLENDE_B3 + BCT_A5 + LIQUID

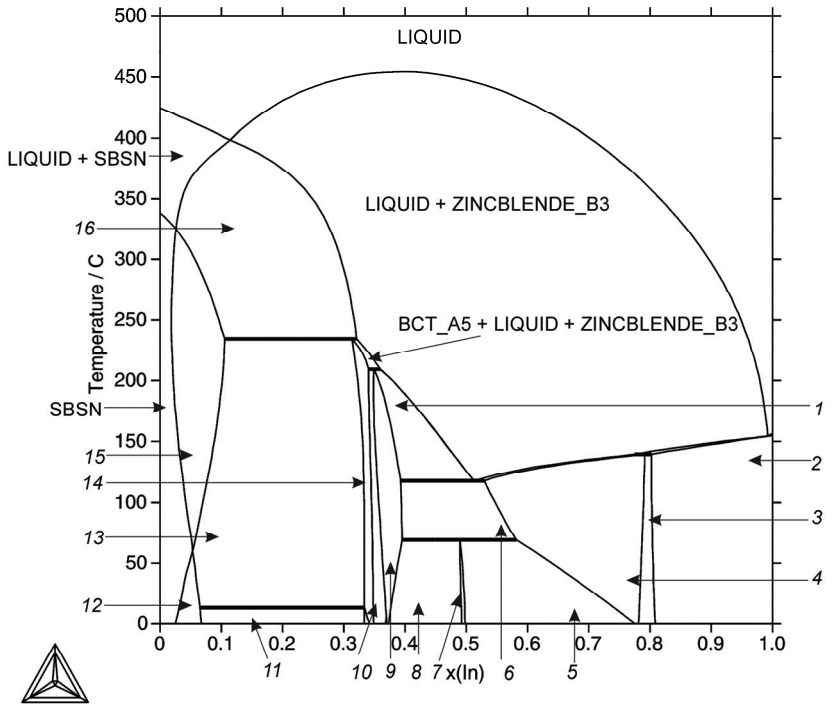

Fig. 213: Isopleth of the In-Sb-Sn system with the ratio Sb:Sn of 1:1

Legend:

1 – ZINCBLENDE_B3 + INSN_GAMMA + LIQUID
2 – ZINCBLENDE_B3 + TETRAG_A6
3 – ZINCBLENDE_B3 + TETRAG_A6 + TET_ALPHA1
4 – ZINCBLENDE_B3 + TET_ALPHA1
5 – ZINCBLENDE_B3 + TET_ALPHA1 + SBSN
6 – ZINCBLENDE_B3 + TET_ALPHA1 + INSN_GAMMA
7 – ZINCBLENDE_B3 + TET_ALPHA1 + INSN_GAMMA
8 – ZINCBLENDE_B3 + INSN_GAMMA + SBSN
9 – ZINCBLENDE_B3 + INSN_GAMMA
10 – ZINCBLENDE_B3 + INSN_GAMMA +BCT_A5
11 – ZINCBLENDE_B3 + SBSN + DIAMOND_A4
12 – DIAMOND_A4 + SBSN
13 – ZINCBLENDE_B3 + SBSN + BCT_A5
14 – ZINCBLENDE_B3 + BCT_A5
15 – ZINCBLENDE_B3 + SBSN
16 – ZINCBLENDE_B3 + SBSN + LIQUID

In-Sn-Zn System

The data from Cui *et al.* **[01Cui]** when combined with the current binary data were found to give good agreement with experimental data and were therefore adopted for the COST 531 database.

References:

[01Cui] Cui, Y., Liu, X. J., Ohnuma, I., Kainuma, R., Ohtani, H., Ishida, K.: *J. Alloys and Compounds*, 2001, **320**, 234-241.

Table of invariant reactions

T / °C	Reaction type	Phases	Compositions		
			x_{In}	x_{Sn}	x_{Zn}
183.6	U1	LIQUID	0.105	0.793	0.102
		BCT_A5	0.040	0.954	0.006
		HCP_ZN	0.000	0.001	0.999
		INSN_GAMMA	0.067	0.933	0.000
122.6	U2	LIQUID	0.775	0.196	0.029
		TETRAG_A6	0.827	0.169	0.004
		HCP_ZN	0.001	0.000	0.999
		TET_ALPHA1	0.818	0.182	0.000
106.0	E1	LIQUID	0.527	0.449	0.024
		HCP_ZN	0.000	0.000	1.000
		INSN_GAMMA	0.230	0.770	0.000
		TET_ALPHA1	0.575	0.425	0.000

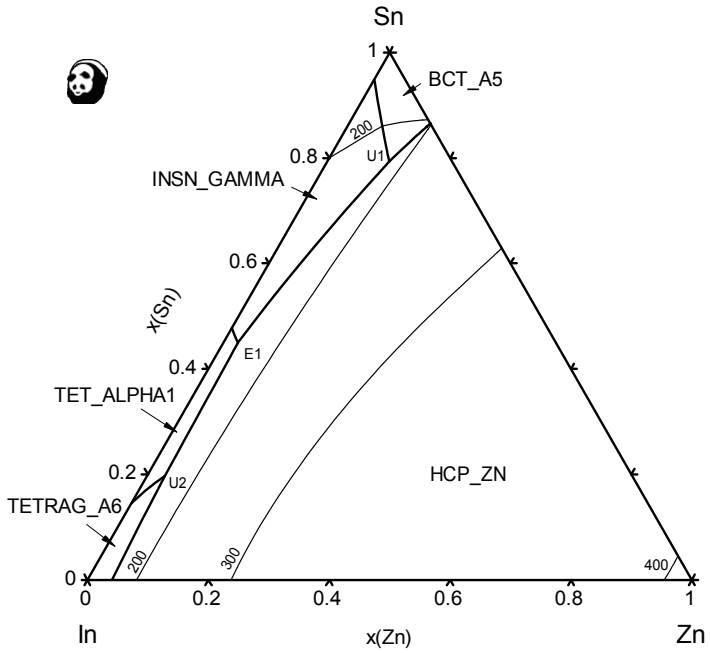

Fig. 214: Liquidus projection of the In-Sn-Zn system

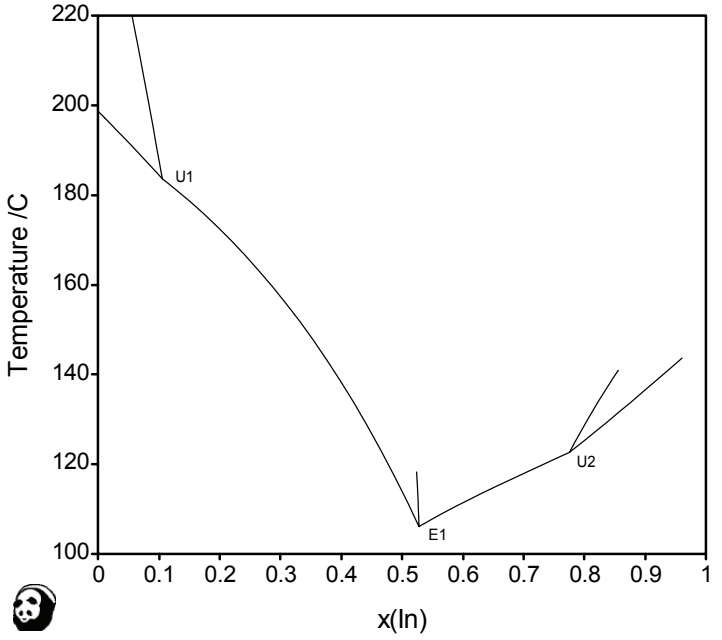

Fig. 215: Liquidus lines in the In-Sn-Zn system in the region of the low-temperature invariants projected onto the T- x(In) plane

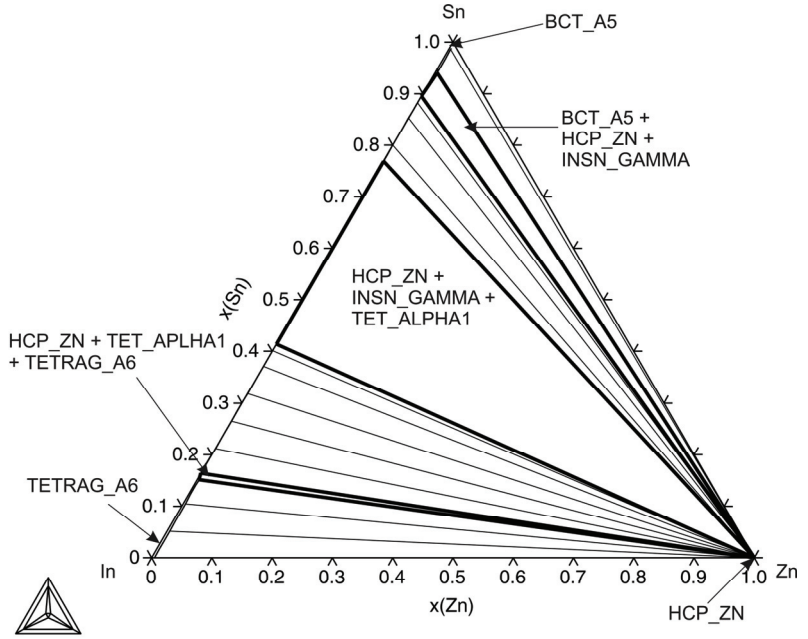

Fig. 216: Isothermal section at 100 °C

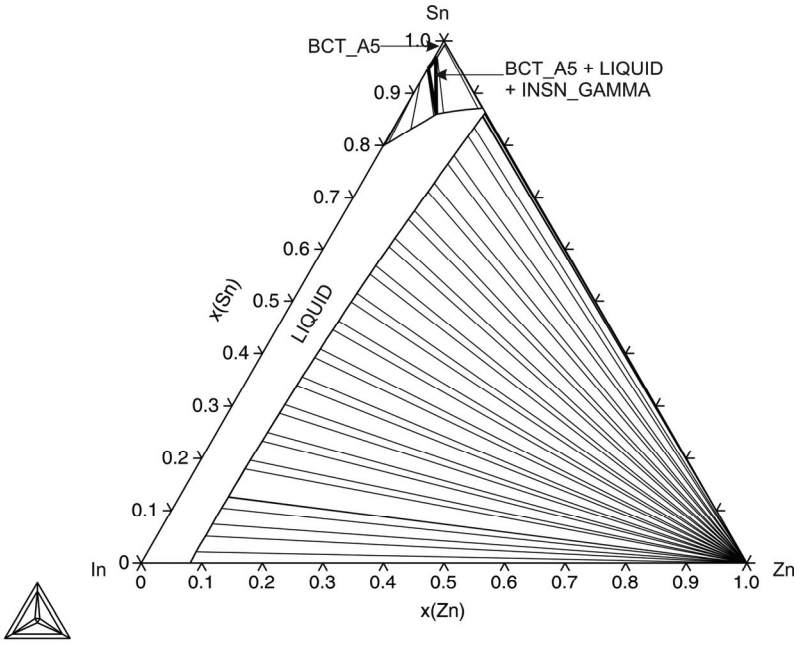

Fig. 217: Isothermal section at 200 °C

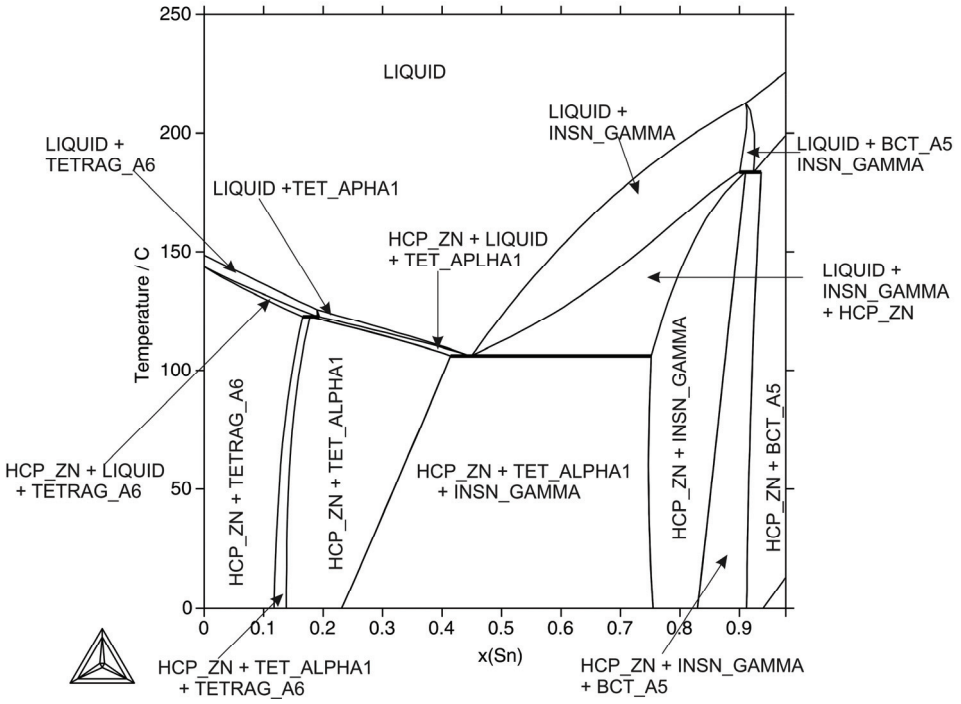

Fig. 218: Isopleth of the In-Sn-Zn system for 2.4 at% Zn (near the invariant point E1)

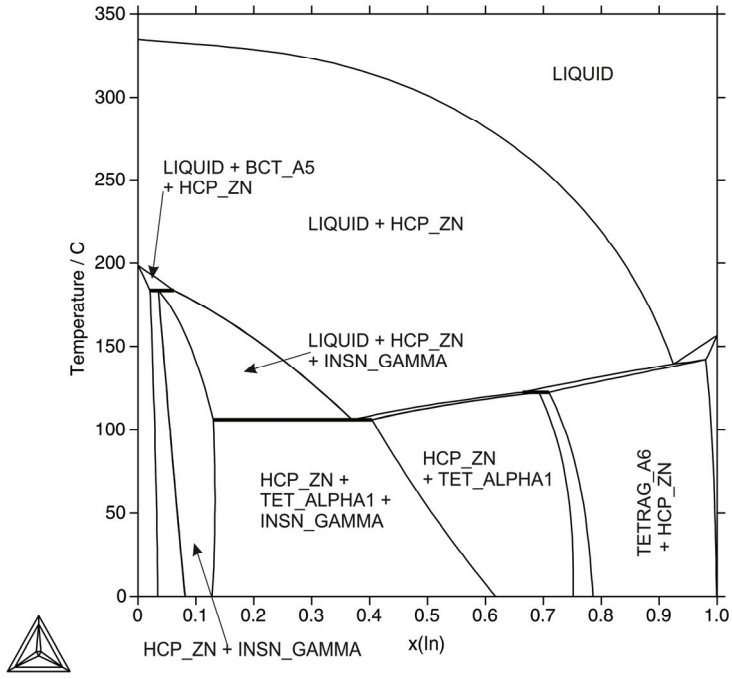

Fig. 219: Isopleth of the In-Sn-Zn system with the ratio Sn:Zn of 1:1

4 – Appendix

Table of Crystallographic Structures